Arab J Sci Eng (2018) 43:43–61
https://doi.org/10.1007/s13369-017-2835-1

REVIEW ARTICLE – BIOLOGICAL SCIENCES

Synthesis, Characterization and Applications of Magnetic Iron Oxide Nanostructures

Ibrahim Khan[1,2] · Amjad Khalil[3] · Firdous Khanday[3] · Ahsan Mushir Shemsi[4] · Ahsanulhaq Qurashi[1,2] · Khawar Sohail Siddiqui[3]

Received: 21 May 2017 / Accepted: 2 October 2017 / Published online: 24 October 2017

Abstract Magnetic iron oxide nanoparticles (MIONPs) have been extensively utilized for several applications that include catalysis (artificial enzymes, nanozyme), renewable energy harvesting, solvents detoxification, heavy-metal remediation, biosensors and medical biotechnology such as drug delivery and magnetic resonance imaging. The magnetic susceptibility of iron oxide nanoparticles (IONPs) is the key feature, which enables them to be utilized for these applications. Depending on specific applications, various experimental methods like hydrothermal, sol–gel, co-precipitation, physical (PVD), and chemical vapor deposition (CVD) can be employed for the fabrication of MIONPs of desired properties. This review critically discusses various techniques for the synthesis and characterization of MIONPs, and their key applications in the fields of health, environment, agriculture, energy, and industrial sectors. The review is concluded with suggestions for future research with a view to efficient utilization and technological applications of MIONPs.

✉ Amjad Khalil
amjadb@kfupm.edu.sa

✉ Ahsanulhaq Qurashi
ahsanulhaq@kfupm.edu.sa

1 Center of Research Excellence in Nanotechnology, King Fahd University of Petroleum and Minerals (KFUPM), Dhahran 31261, Saudi Arabia

2 Department of Chemistry, KFUPM, Dhahran 31261, Saudi Arabia

3 Life Sciences Department, KFUPM, Dhahran 31261, Saudi Arabia

4 Center for Environment and Water, KFUPM, Dhahran 31261, Saudi Arabia

Keywords Energy harvesting · Nanoparticles · Nanotechnology · Environmental remediation · Health · Industry · Agriculture

1 Introduction

Nanostructure materials possess exceptional optoelectronic properties due to quantum effects that manifest at small sizes (1–100 nm). Nanomaterials are predominantly used as catalysts for a variety of applications that include but is not limited to water splitting, gas sensing, heavy-metal detection, biosensors, and dye degradation [1–6].

Since early 2000, extensive research has been carried out on the synthesis of magnetic iron oxide nanoparticles (MIONPs) for various technological applications like sensing, catalysis, photocatalysis, drug delivery, and storing data. Initially most of the researchers used it in biosensing [7] and other medical applications such as drug delivery [8], magnetic resonance imaging (MRI) [9] and contrast agents [10] owing excellent magnetic characteristics. Furthermore, MIONPs were also utilized in jet printing inks [11,12]. More recently MIONPs found substantial applications in catalysis as a catalyst in pristine and modified forms [13–15]. They are also emerging in the field of energy harvesting as well [16,17].

Iron oxides are easily available, inexpensive, and nontoxic materials, with abundant distribution in nature in the forms of various ores. Iron oxide compounds can also be synthesized artificially via various physicochemical techniques like co-precipitation, thermal decomposition, hydrothermal, and solvothermal methods and sol–gel technique [18–22]. Certain oxides of iron (such as hematite, Fe_2O_3, magnetite, and Fe_3O_4) possess magnetic susceptibility and other unique properties (catalytic, photoactive, and mechanical), due to

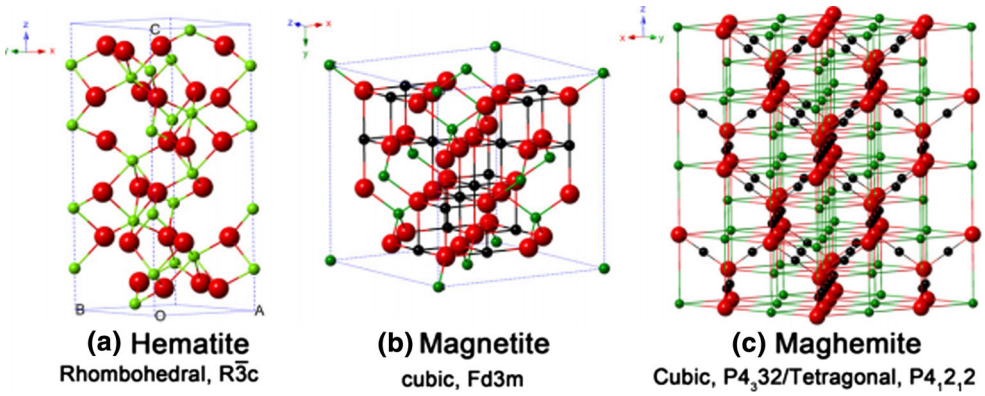

Fig. 1 Crystal phases of iron oxide with space group details [23]

which these can be utilized in a variety of applications in the field of energy harvesting, environmental bioremediation, catalysis, agriculture and health. Iron oxides exist in various crystal forms as shown in Fig. 1 [23].

Hematite and magnetite predominately possess magnetic characteristics and exist is rhombohedral and cubic forms, respectively (Fig. 1a, b).

Fe_2O_3 is existed in α-Fe_2O_3, β-Fe_2O_3, γ-Fe_2O_3, and ε-Fe_2O_3 polymorph forms [24]. The abundantly existed α-Fe_2O_3 (hematite) is existed in rhombohedral crystal unit, while the γ-Fe_2O_3 (maghemite) is found as tetragonal crystal phase (Fig. 1a, c), while the β-Fe_2O_3 and ε-Fe_2O_3 polymorphs can be synthesized and exist as cubic bixbyite and orthorhombic structures respectively. ε-Fe_2O_3 polymorph is a transition phase between hematite and maghemite. The magnetic properties of these polymorphs are related to their structures, and therefore, α-Fe_2O_3 is canted antiferromagnetic, β-Fe_2O_3 is paramagnetic, and γ-Fe_2O_3 and ε-Fe_2O_3 are ferromagnetic [24–26].

Compared to other oxides, magnetite (Fe_3O_4) is unique as it possesses both divalent (Fe^{2+}) and trivalent (Fe^{3+}) forms of iron. It has a cubic inverse spinel structure, where Fe^{2+} ions inhabit half of the octahedral sites, while Fe^{3+} are fragmented consistently across remaining octahedral and tetrahedral sites. Fe_3O_4 exist as both n- and p-type semiconductor with a very small band gap of 0.1 eV.

Table 1 provides comparison of the physiochemical properties of different forms of iron oxide. In addition to these forms, iron oxide also exists in nonstoichiometric black powder form, which is iron(II) oxide (FeO). FeO is existing in wustite mineral form having cubic crystal structure [27,28].

Though the cubic structure changes with decrease in temperature and become rhombohedral phase below 200 K, which alters their behavior to anti ferromagnetic characteristic [28]. FeO used as figment in many cosmetics applications, e.g., tattoo inks [28]. Due to such exceptional characteristics and wide ongoing research, we opt to provide some comprehensive discussion about the recent trends in the synthesis and applications of MIONPs with suitable literature review. This review will be significant addition to the literature for the readers in the related field.

2 Size, Shape and Magnetic Properties

Out of the different polymorphs of Fe_2O_3, α-Fe_2O_3 acquires lower ferromagnetism at room temperature with saturation magnetization less than 1 emu/g. In contrast, γ-Fe_2O_3 displays strong ferrimagnetism like Fe_3O_4 at room temperature, with saturation magnetization that can approach 92 emu/g [30]. The properties of MIONPs depend on size and shape of nanomaterials that can be tuned via different synthetic techniques. Ceylan et al. established the effect of size on the magnetic properties of iron/iron oxide core shell structured NPs. They concluded that the small NPs show super paramagnetic behavior and also exhibit high exchange bias field [31]. Therefore, MIONPs ranging from 13 to 18 nm, showed excessive magnetic disorder due to severe loss of their hyperthermia performance [32]. Guardia et al. demonstrated the effect of surfactant on the size of MIONPs. They showed that smaller-sized particles (4–20 nm) were obtained when MIONPs were synthesized in the presence of oleic acid surfactant, while the bigger particles (45 nm) were obtained when decanoic acid was used during fabrication [33].

Like size morphology also effects the magnetic behavior of IONPs. One-dimensional (1D) IONPs exhibit different magnetic properties as compared to higher dimensional particles. Recent study revealed that the magnetic properties of single and tubular clustered IONPs varied as a function of morphology. It was demonstrated that the coercively hysteresis changes significantly with the shape of the nanoparticle (Fig. 2a–c) [34].

Table 1 Physiochemical characteristics of IONPs [29]

Property	Oxide		
	Hematite	Magnetite	Maghemite
Molecular formula	α-Fe_2O_3	Fe_3O_4	γ-Fe_2O_3
Density (g/cm^3)	5.26	5.18	4.87
Melting point (°C)	1350	1583–1597	–
Hardness	6.5	5.5	5
Type of magnetism	Weakly ferromagnetic or antiferromagnetic	Ferromagnetic	Ferrimagnetic
Curie temperature (K)	956	850	820–986
M_S at 300 K (A-m^2/kg)	0.3	92–100	60–80
Standard free energy of formation ΔG_t° (KJ/mol)	−742.7	− 1012.6	− 711.1
Crystallographic system	Rhombohedral, hexagonal	Cubic	Cubic or tetrahedral
Structural group	Corundum	Inverse spinel	Defect spinel
Space group	R3c (hexagonal)	Fd3m	$P4_332$ (cubic); $P4_12_12$ (tetragonal)
Lattice parameter (nm)	$a = 0.5034$, $c = 1.375$ (hexagonal) $a_{Rh} = 0.5427$, $\alpha = 55.3°$ (rhombohedral)	$a = 0.8396$	$a = 0.83474$ (cubic); $a = 0.8347$, $c = 2.501$ (tetragonal)

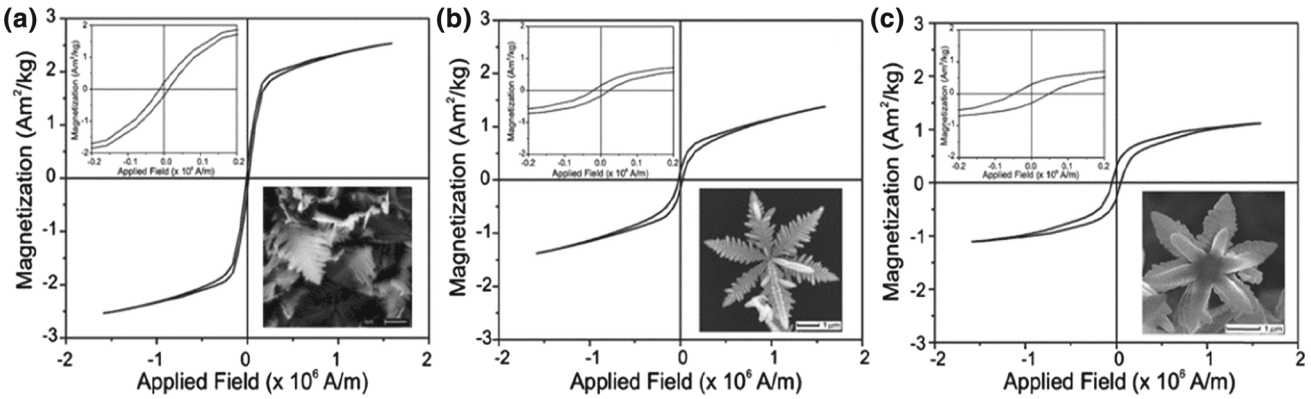

Fig. 2 Room-temperature magnetic hysteresis loops of nanostructured α-Fe_2O_3 with **a** dendritic, **b** single-layered snowflake, and **c** double-layered snowflake morphology. The inset images are the corresponding magnified hysteresis loops and microstructure for each sample (reprinted from ref. [34], Copyright (2010), with permission from the Royal Society of Chemistry)

3 Synthesis of MIONPs

The control in size (1–100 nm) and shape depends on synthetic method used for the fabrication of nanomaterials that in turn governs their properties (mechanical, electrical, magnetic, optical, chemical). These methods are divided into two main types "*Bottom-Up*" and "*Top-Down*". Bottom-up methods involve the compilation of atoms or molecules into larger nanostructured arrays whereas top-down methods involve carving the structure from a larger part manually or by some self-structuring process. The benefits of top-down include cost, scalability and better uniformity of the product whereas bottom-up strategy involves less defects, more homogenous chemical composition, and better short- and long-range ordering [35].

To date, numerous protocols have been adopted for the synthesis of MIONPs. Bottom-up and top-to-bottom techniques are utilized involving both aqueous and non-aqueous reaction media. Generally, aqueous routes are preferred due to being cheaper and sustainable; however, soluble MIONP have certain disadvantages compared to non-aqueous techniques. Various reaction parameters like temperature, pressure, reaction time, and the role of precursors influence the physiochemical properties of the final product. As discussed above, the morphology and particle size influence the magnetic properties, and therefore, synthesis of NPs

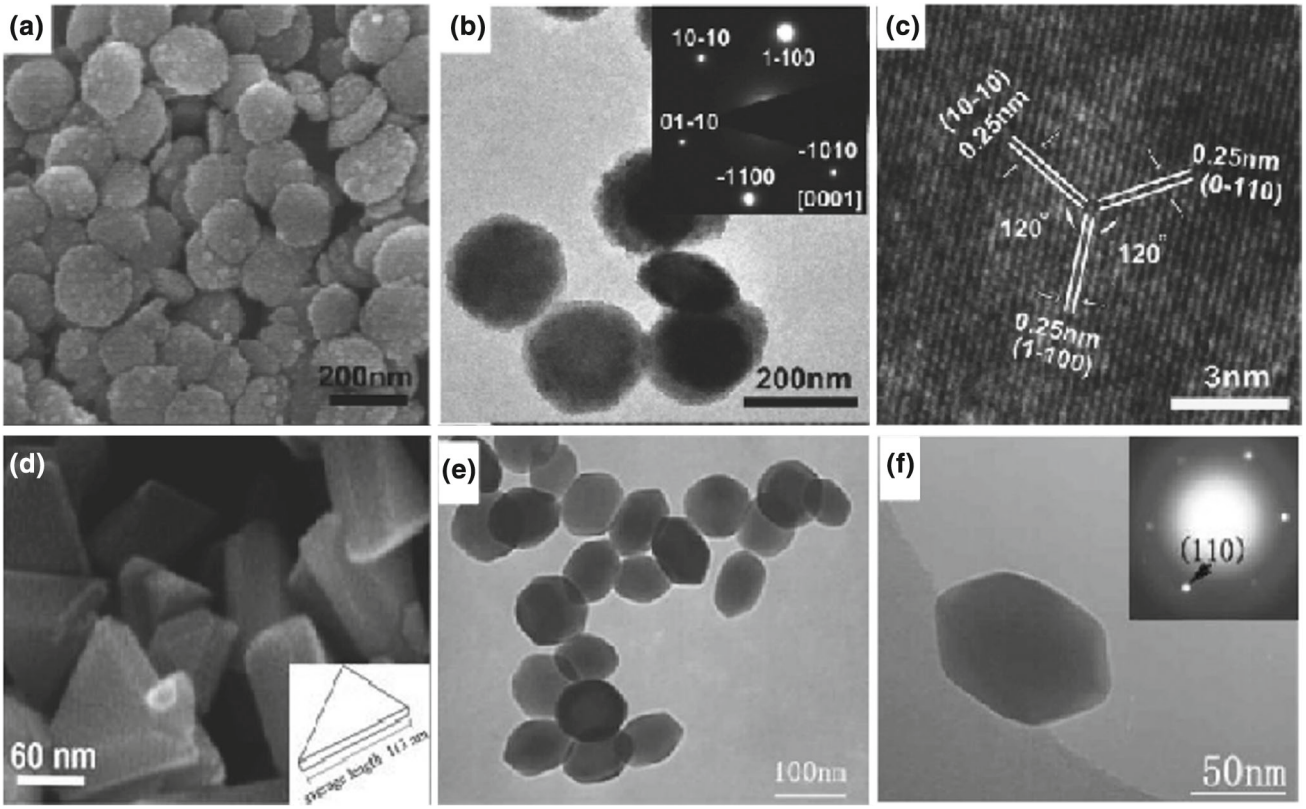

Fig. 3 **a–c** SEM, TEM and HRTEM images of a-Fe_2O_3, **d–e** SEM of Fe_3O_4 triangular nanoprisms and **e**, **f** TEM and SAED pattern of hexagonal Fe_2O_3 nanoplate (reprinted from ref. [36], Copyright (2016), with permission from the RSC)

play a vital role in controlling these parameters. Scanning electron microscopy (SEM) and high-resolution transmission electron microscopy (HRTEM) are the two well-known characterization techniques for revealing the morphologies of nanomaterials at very small scale. As the name implies, the principle of SEM is based on scattered electrons, while TEM is based on transmitted electrons. Figure 3 shows [36] the SEM and HRTEM images of MIONPs, which present different morphologies. In the following sections, some key bottom-up and top-down synthetic techniques for the synthesis of MIONPs of various shapes and sizes are described.

3.1 Wet-Chemical Synthesis

Synthesis using hydrothermal and solvothermal techniques are the most common routes for the fabrication of MIONPs. These techniques are relatively simple, inexpensive, and rapid, and require easily available materials. Most importantly, the particle size and shape can be controlled by varying various reaction parameters. For example, it is reported that the size of IONPs can be manipulated by changing the growth temperature between 60 and 180 °C in addition to the duration of reaction. When the reaction temperature was elevated from 100 to 180 °C for ∼ 12 h, NP size also increased proportionally from ∼ 14.5 to ∼ 29.9 nm. Alternatively, when the reaction time was varied from 1 to 48 h at a constant temperature (180 °C), NPs size increased from ∼ 20.6 to ∼ 123 nm [23]. Similarly, Riasat et al. developed α. Fe_2O_3 NPs by using simple hydrothermal strategy. The highly crystalline nanosphere-shaped NPs were obtained at 180 °C with 24 h reaction time [37]. Furthermore, the hydrothermal/solvothermal route is also critical in controlling shape of MIONPs. For example, the anion-assisted hydrothermal/solvothermal technique has been adopted for the synthesis of short nanotubes and ring-shaped MIONPs [20].

3.2 Co-precipitation

Like hydrothermal, co-precipitation technique is well established for the synthesis of large-scale MIONPs. The pH and nucleation steps are critical in this method, and they must be controlled precisely in order to obtain the desire product. In a typical experiment, Khalil et al. used single iron(III) salt precursor to obtain magnetite NPs by keeping the 2:1 mole ratio of Fe(III) and Fe(II) at pH 9–11. The NPs obtained under these conditions were elongated rod shaped [38]. Similarly, Wu et al. [39] adopted Scheme 1 to synthesize

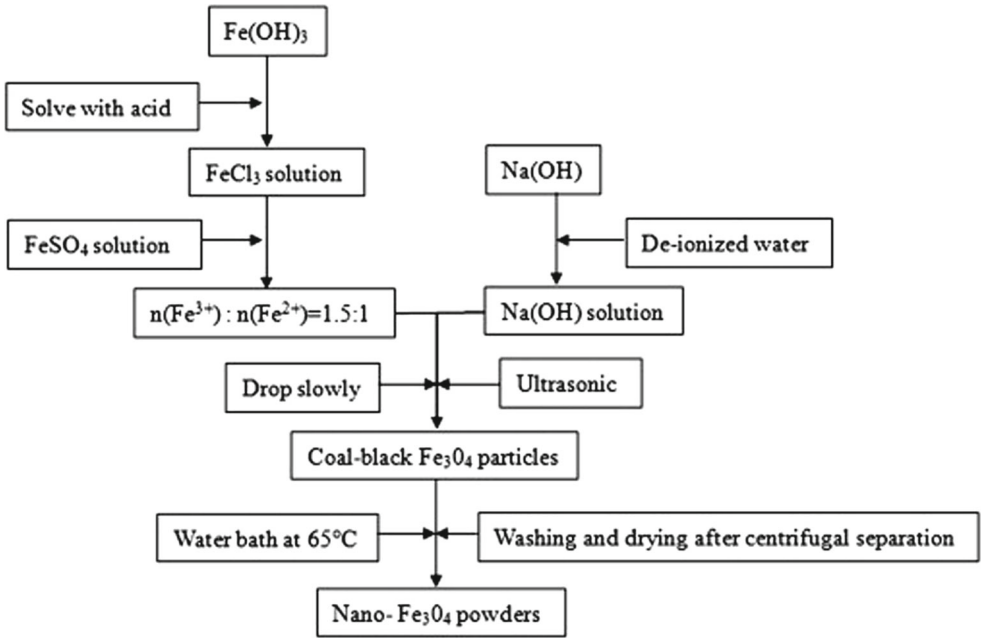

Scheme 1 Synthesis protocol for Fe_3O_4 NPs preparation via co-precipitation [39]

MIONPs nanopowders (15 nm) by ultrasonic-assisted modified co-precipitation technique followed by acid leaching to get high purity MIONPs. The MIONPs obtained by this technique showed high saturation magnetization and precise morphology; however, the employment of strong bases and surfactant limit its productivity.

3.3 Sol–Gel and Related Method

Like above two methods, it is a classical wet-chemical technique widely utilized for the synthesis of inorganic metal/semiconductor oxide NPs with an advantage to manipulate their shape. This technique involves two phase aqueous media, the liquid (sol) and gel and requires the presence of a surfactant in the parent solvent. The sol is a stable dispersion, whereas the gel consists of three-dimensional continuous network that forms micelles around the liquid phase. Physical forces such as Van der Waals and hydrogen bonds are dominant in the sol–gel media. For the synthesis of MIONPs, the prominent precursors include iron alkoxides and other iron salts, which undergo a series of hydrolysis and condensation reactions to form the final product [40], where the overall properties of MIONPs depend on their structure.

Using Fe(III) acetylacetonate precursor via benzyl alcohol route, crystalline MIONPs were obtained, ranging in size from 5 to 15 nm [41]. By employing a similar technique, MIONPs with an average size of 8 nm were obtained by Lemine et al. with saturated magnetization that reached 47 emu g^{-1} [42]. Compared to traditional hydrothermal/solvothermal method, sol–gel method can be performed at lower pressures and therefore does not require autoclave vessel. Additionally, this method produces highly dispersed NP with precise size control; however, the method is limited by its high cost, unsafe operating conditions, and longer reaction times.

3.4 Dry Synthesis Techniques

Compared to wet synthesis, dry or thermal decomposition methods produce more precise particle size. These methods are divided into hot-injection and conventional reaction approaches. Temperature is the most critical driving force in these methods as it governs most of the properties of the final product. Generally, highly monodispersed and crystalline MIONPs are obtained by high-temperature (above 400 °C) dry techniques. MIONPs resulting from these methods are usually soluble in nonpolar solvents and have exceptional physical characteristics such as high mechanical strength and optical properties. Recently, Unni *et al.* synthesize MIONPs via thermal decomposition technique with controlled magnetic properties by employing organometallic precursors of iron. They further studied the effects of structural defects on the overall magnetic behavior of MIONPs [43]. Although this technique produces high-quality MIONPs, the high cost and elevated temperature are the major concerns.

3.5 Microwave-Assisted Synthesis

Excitation via electromagnetic radiation is a well-known phenomenon, and this process can be used effectively for

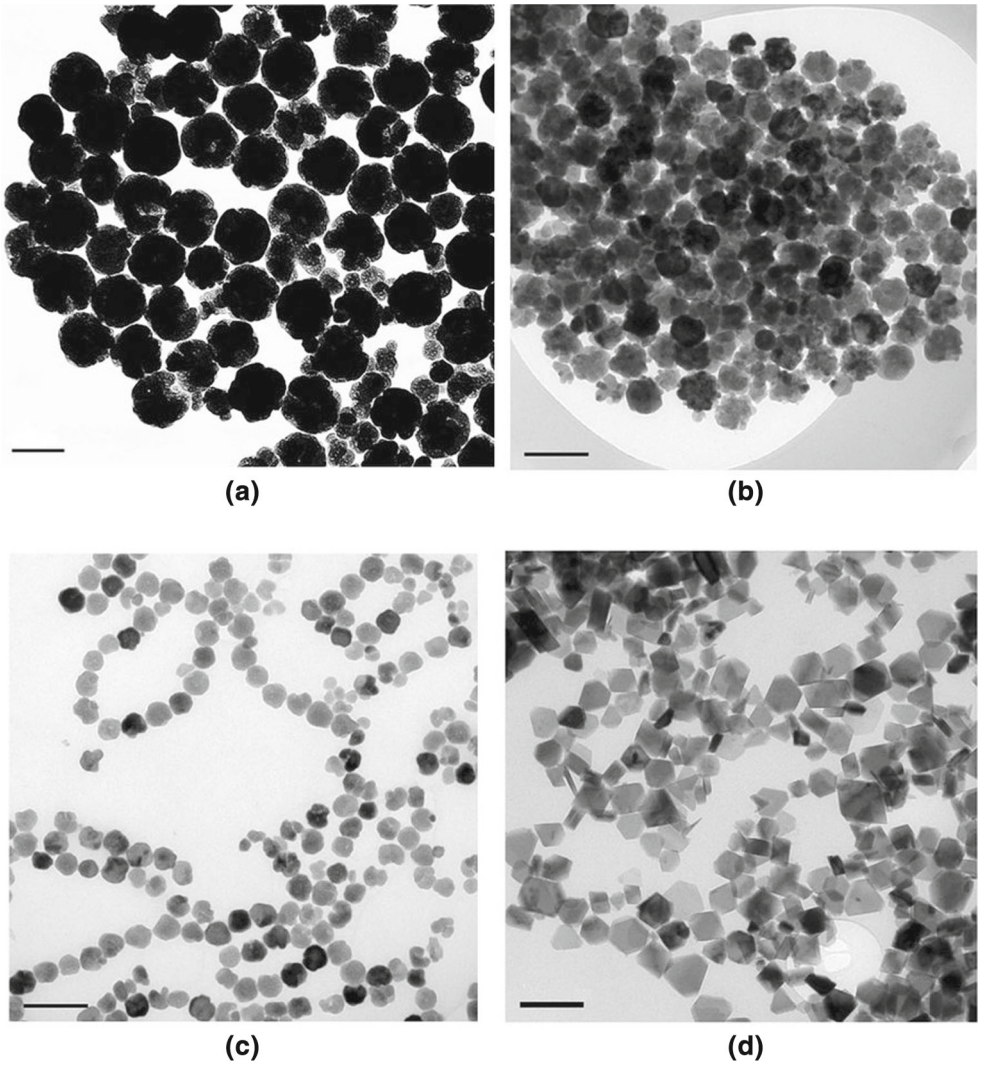

Fig. 4 TEM images of MIONPs: **a** 180 nm particles (DEG/EG = 0/40); **b** 100 nm particles (DEG/EG = 26/14); **c** 60 nm particles (DEG/EG = 30/10); **d** nanosheets (DEG/EG = 40/0) [46]

the synthesis of NPs. Radiation in the microwave range is known for its heating effect in household ovens and can be used for the synthesis of various nanomaterials especially the MIONPS. Large-scale yields can be achieved in limited time due to strong homogenous heating capacity of the microwave radiation. MIONPs have been synthesized by a simple, rapid solvothermal method from $FeCl_3 \cdot 6H_2O$ precursor, ethylene glycol (EG) solvent, and a nucleating agent. With a synthesis time of only 30 min in pressurized microwave reactor, 20–130 nm-sized NPs were obtained with uniform shape and excellent magnetic properties (saturation magnetization, 8–76 emu g^{-1}) in high yield that approached 100% [44].

3.6 Ultra-sonochemical Synthesis

Like microwave, synthesis by ultrasonic methods also follow similar principle. These rays originate from a well-known acoustic cavitation effect with very high intensity and produce immense heat inside the reaction medium. Acoustic waves are composed of alternate expansion and compression waves, which make bubbles or cavities to oscillate. These oscillating bubbles conserve ultrasonic energy and release the energy on its collapse [45]. The sonolysis method is successfully used by researchers to prepare MIONPs of various shapes and functionalities. Preparation of MIONPs having nanosheet morphology was achieved with exceptional magneto-chromatic properties via ultrasonic-assisted solvothermal method. The molar ratio of diethylene glycol (DEG) and ethylene glycol (EG) was the key in controlling the shape of the MIONPs. Figure 4 shows a TEM images of MIONPs obtained via this technique having various sizes and shapes [46].

4 Applications of MIONPs

4.1 Energy-Harvesting Applications

MIONPs have significant applications in the field of energy harvesting. These NPs have been utilized in various energy-related fields like water splitting, photovoltaic solar cells, and CO_2 conversion to value-added products.

4.1.1 Water-Splitting Applications of MIONPs

Water splitting is a topical research area due to its potential to substitute the traditional energy sources that are mainly based on fossil fuel with concomitant reduction in CO_2 emissions. For this purpose, semiconductor materials have been widely employed [47–53]. These materials possess unique optical properties like suitable band gap (1.5–2.5 eV), band edge positions, low charge recombination, and high interfacial charge transfer abilities. Owing to unique optical characteristics, MIONPS have also been investigated substantially by various research groups for photoelectrochemical (PEC) water-splitting applications to generate oxygen and hydrogen. MIONPs emerged as a promising photoactive material due to various functionalities like substantial light absorption, ample abundance and most importantly, chemical stability in a variety of aqueous media. Sivula *et al.* have provided a thorough overview on the PEC water-splitting applications of MIONPs, especially the hematite (α .Fe_2O_3 form) [54]. Bare hematite thin films were prepared by sophisticated spray pyrolysis approach by optimizing various parameters such as sprayed volume of solution, temperature, and time gap between sprays. The PEC water-splitting measurements show a photocurrent density of $\sim 0.94\,mA/cm^2$ at 1.45 V, with extreme stability of > 1000 h under 1-SUN simulated sunlight [17]. Similarly, the Fe_3O_4/FeO photoanodes were designed for PEC water splitting, that exhibited hydrogen production in two cycles. Cycle (i) involved endothermic PEC reduction in the magnetite (Fe_3O_4) at a relatively high temperature and cycle (ii) involved the exothermic steam hydrolysis of wustite (FeO) for hydrogen generation. Significant (83%) hydrolysis conversion was attained for both cycles at 575 °C [55]. However, the PEC water-splitting performance of pristine MIONPs is somehow limited by high recombination of charges (holes and electrons) and photocorrosion in acidic or basic media. In order to overcome these limitations, NPs are engineered in different ways to obtain an efficient and resilient photocatalyst. These include precise control of size and morphology during synthesis, doping, nanocomposite formation, etc. For example, The O/Fe ratio in MIONPS can be fine-tuned by creating oxygen vacancies to improve PEC properties of these materials as reported by Rioult et al. By using thermal hematite reduction and magnetite oxidation, they obtained semiconducting MIONPs with controlled stoichiometries for solar water splitting. They achieved a substantial reduction of 0.2 V for the onset potential and an overall photocurrent increase of 50% with respect to stoichiometric hematite [16]. Similarly, another group reported MIONPs based on zirconia composite for PEC water splitting with improved hydrogen generation capacity due to the hybrid formation [56].

4.1.2 MIONPs Comprised Photovoltaic (PV) or Dye-Sensitized Solar Cells (DSSCs)

Photovoltaic (PV) cells are well known for their solar energy generation potential. These cells are normally made of organic and inorganic counter parts, where MIONPs can be employed as a suitable candidate for the inorganic part. Recently, due to their industrial successes, DSSCs have represented the third generation of specialized solar cells that have gained universal attention [57]. They are an exceptional candidate for the storage of clean energy. Generally, DSSC consists of a dye-sensitized photoanode, an electrolyte (redox couple, e.g., I^-/I^{3-}) and a counter electrode. Anatase TiO_2 photoanode was initially employed for DSSCs but abandoned due to large band gap (3.2 eV) that was unable to adsorb the visible part of the electromagnetic radiations, with concomitant decrease in its efficiency [58]. Therefore, many semiconductor materials were tested to substitute TiO_2. Due to narrow band gap, α-Fe_2O_3 films have also been investigated, which showed good photovoltaic performances in DSSCs [59]. MIONPs absorb significantly in the visible region and therefore can provide more sites due to high surface area. As discussed before, the morphology of DSSCs critically influences the physicochemical properties of the nanomaterials such as photon-to-electron conversion efficiency. For example, α-Fe_2O_3 nanorod arrays (NRAs) and NPs showed different conversion efficiencies, i.e., 0.43, and 0.29%, respectively [60]. More interestingly, MIONPs can also be efficiently used as a counter electrode as they can effectively trap electrons from external circuit [61]. For example, nanoflower-shaped hierarchical structured Fe_3O_4 synthesized for DSSCs have been used as the counter electrode (Fig. 5) [62], which showed a power conversion efficiency of 7.65% compared to the efficiency of pyrolytic Pt (6.88%) and sputtered Pt (7.87%).

4.2 MIONPs in CO_2 Conversion Applications

Carbon dioxide emissions produced by thermal power stations, chemical, cement and petrochemicals industries, refineries, and exhaust fumes are believed to be the cause of global warming, and their recycling to harvest carbon-neutral solar fuels can be a potential path to decrease CO_2 emissions [63]. Therefore, researchers are trying to develop

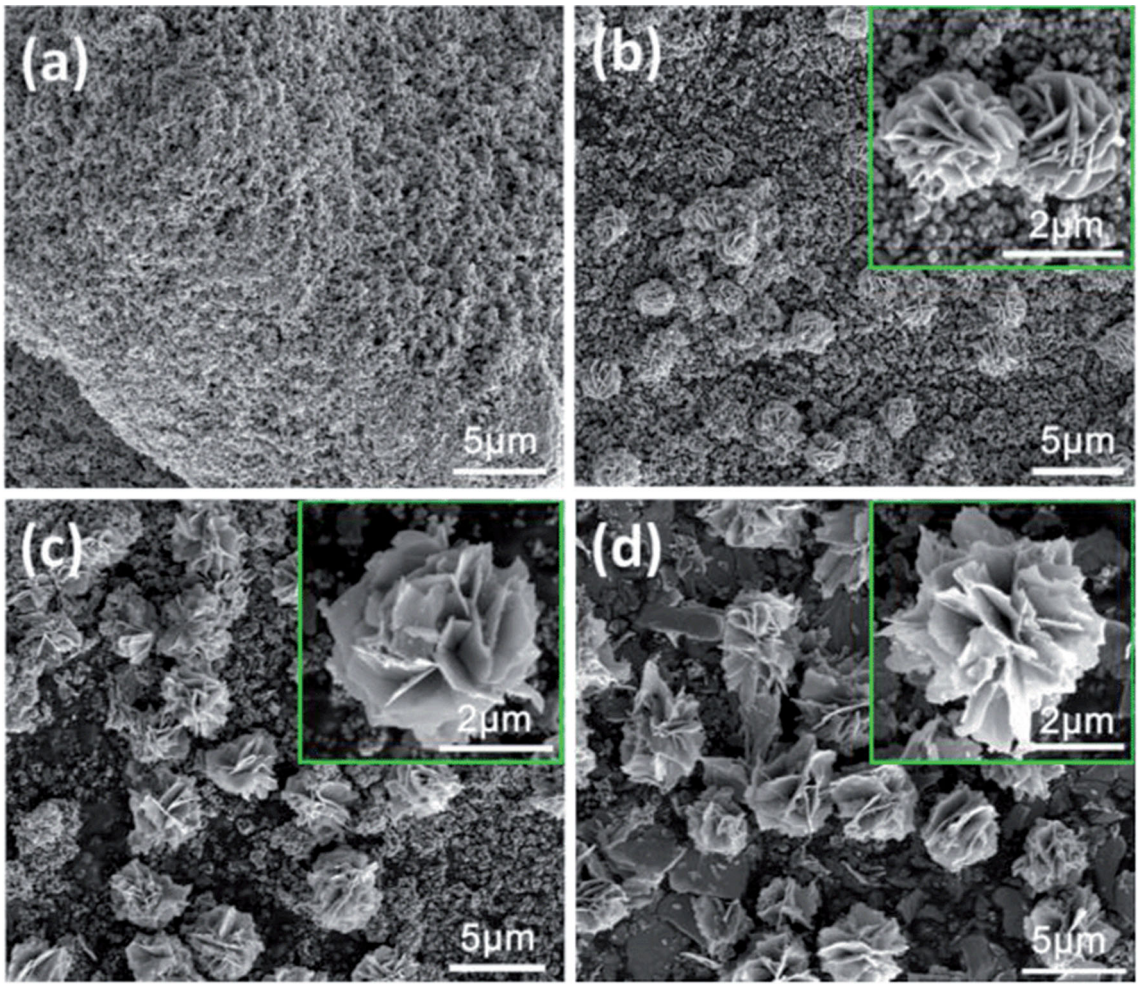

Fig. 5 The SEM images of the flower-like Fe_3O_4 at different temperatures **a** 165 °C, **b** 175 °C, **c** 185 °C and **d** 195 °C [62]

technologies that can trap/capture and convert CO_2 into another useful form, such as a fuel [64]. The photoelectrochemical or electrochemical modification of CO_2 into CO offers many significant advantages, e.g., to obtain valuable fuel in the form of organic gases, fossil fuels savings, solar energy storage into chemical energy, manufacturing of other products like liquid gas, etc. Therefore, MIONPs can be effectively used to serve as catalyst for the conversion of CO_2 into value-added products. The solar-induced splitting of CO_2 into CO by facile thermochemical looping via Fe_3O_4/FeO redox reactions has been achieved. The two-step process involves reactions similar to water splitting as discussed above, i.e., (i) the endothermic reduction of Fe_3O_4 to FeO and O_2 through intense solar energy, and (ii) the non-solar exothermic oxidation of FeO with CO_2 to generate CO. FeO conversion higher than 90% can be achieved with high reaction rates depending on temperature, particle size, and CO_2 concentration [65]. Similarly, Fan et al. [66] reported the conversion of CO_2 to diphenyl carbonate (DPC) via $ZnBr_2$ supported on silica-coated Fe_3O_4 NPs in the presence of CCl_4 with an efficiency of 28% of DPC yield under optimum conditions.

4.3 Application of MIONPs in Catalysis

The development, improvement, and utilization of heterogeneous catalysis is recently been in great demand due to its easy separation, recovery and reuse because separation and recycling of homogeneous catalysts is difficult and uneconomical. In order to achieve easy separation and recycling, numerous industrial homogeneous catalysts have been immobilized on different solid supports including iron-based magnetic nanostructures. Under industrial settings, the advantage of magnetic catalysts is their facile recovery after the reaction by the application of an external magnetic field. This makes magnetic nanoparticles (MNPs) practical, cost-effective, and environmental friendly. There are numerous MNPS based on cobalt, nickel, iron and oxides of iron and ferrite. Among these, MIONPs are widely exploited as heterogeneous catalysts due to their simple and rapid prepara-

tion, non-toxic nature, and inexpensiveness. Depending upon the specific application, MIONPs of required size, shape, and magnetic properties are synthesized as described in Sect. 2. Several types of magnetic nanostructures and composites have been developed for use in catalysis [67,68]. The catalytic activity of pristine MIONPs can be further enhanced via coating or composite formation with other materials, such as silica, polymers, and metals.

Zolfigol et al. [69,70] synthesized a composite imidazole-based ionic liquid-stabilized silica-coated Fe_3O_4 MNPs [nano-Fe_3O_4-SiO_2-$(CH_2)_3$-imidazole-SO_3H]Cl as a novel heterogeneous acidic catalyst. This catalyst was used for the synthesis of 1,8-dioxooctahydroxanthene and dihydropyrano [2,3-c]pyrazole derivatives at high temperature under solvent-free conditions.

Similarly, MIONPs-bonded enzyme (lipase from *Aspergillus niger*), catalyst was synthesized and used in the synthesis of benzothiazepine and spirobenzothiazinechroman derivatives through three-component reaction between coumarine-3-carboxylic acid derivatives, 2-aminothiophenol, and alkyl isocyanides at room temperature under mild conditions [71]. Magnetite with a coating of silica doped with copper–salen complex inside the shell was used to catalyze the synthesis of substituted 1- and 5-tetrazoles in high yield [72]. The above-mentioned magnetite support loaded with chromium (IV) was used for the synthesis of 1,1-diacetals from aldehydes [73]. The surface of silica-coated MIONPs catalyst was functionalized with sulfonic acid for the production of 1,8-dioxooctahydroxanthene derivatives in high yield [74].

A novel application of MIONPs with silica shell as a support for manganese or iron containing metalloporphyrin was reported by Nakagaki et al. [75]. These catalysts were utilized for the oxidative reactions of cyclooctene, cyclohexene, and cyclohexane to their respective alcohols. These NPs showed greater selectivity for the conversion of cyclohexane to an alcohol than free metalloporphyrin. Similarly, Abdolalian et al. [76] loaded molybdenum (IV) on a MIONP with a mesoporous silica shell that catalyzed the epoxidation of olefins in the presence of hydrogen peroxide. The epoxidation of cyclooctene, 1-octene, indene, and 1-methylcyclohexene was carried out with a high conversion rate and can be reused up to six cycles.

Hetrogenization of many homogeneous metal-coated or doped catalysts have also been exploited for high-temperature applications for downstream processing of petroleum. The synthesis and industrial applications of these catalysts in high-temperature water gas shift reaction (HTSR) and biofuel production have been widely exploited [77–79]. These catalysts exhibited high CO conversion with increasing molar steam: dry gas ratio. Moreover, carbon-encapsulated iron NPs (CEIN) have been prepared from iron(II) chloride and wood-derived sugars under hydrothermal carbonization (HTC) conditions. The nanospheres thus obtained were approximately 100–150 nm in diameter with an iron core diameter of 10–25 nm. These catalysts were used to thermochemically convert wood-derived syngas into liquid hydrocarbons (Fischer Tropsch synthesis). These NPs showed excellent catalytic performance at 290 °C and biomass-derived syngas conversion of CO (up to 89.5%) and selectivity of 65% [80–82].

It is noteworthy that different morphologies of magnetic Fe_2O_3 nanocrystals, e.g., rhombohedra, truncated rhombohedra and hexagonal sheet effect reduction rates of H_2O_2. These morphologies are very much influenced by different synthesis conditions such as solvent types, temperature, and pH. A template free hydrothermal synthesis of α-Fe_2O_3 hexagonal sheets showed high electrochemical reduction of H_2O_2.X. Li *et al.* [83].

Rafie et al. studied the influence of external electromagnetic field (EMF) to synthesize high-quality and highly active one-dimensional (1-D) Fe_3O_4 nanostructures. The intensity of EMF was varied to critically control the transcription of structural features such as morphology, particle size, pore size distribution and magnetic properties. These catalysts were used under the influence of EMF that affected the rates in the preparation of a series of alkyl-, aryl-, and heteroaryl-substituted imidazoles from the corresponding benzoin and benzyl derivatives [84].

Magnetic property of IONPs is applied in drug delivery and phase contrast agent [85–87] in magnetic resonance imaging [88]. MIONPs that exhibit superparamagnetic behavior above body temperature are potential candidates due to the absence of magnetic remanence and exhibit fast changes in the magnetic state in an applied magnetic field [89]. Particles less than 15 nm have shown mono domain of a uniform magnetization state [90]. Spherical-shaped NPs are better drug carriers and safer than ellipsoid, hexagonal, and cubical MNPs [89]. Successful synthesis of controlled size and shape of iron magnetic nanoparticles using homogeneous co-precipitation and urea thermal decomposition under induced cavitation by sonication has already been discussed. These nanoparticles have shown targeted drug distribution with low toxicity [91].

4.4 Agriculture

In the last two decades, iron-based metallic nanomaterials have fascinated a large number of scientists and have rapidly expanded into diverse fields of research. This huge interest is mainly due to a number of valuable properties these materials have exhibited that have led to new avenues in the field of agricultural nanotechnology. These materials can be synthesized and modified with appropriate functional groups that allows them to process various substances derived from agricultural activities.

Although different types of metal-based (Fe, Ti, Ce, Au, Co, Ni, and Zn) particles have been studied in the last decade; however, iron-based (Fe_2O_3 and Fe_3O_4) NPs generated most interest due to its inexpensive and non-toxic properties. The recent advances in the area of nanotechnology allowed synthesizing a wide range of novel and low-cost MIONPs with very exciting properties that assisted and outlined the next stage of development of plant and animal biotechnology, pesticides, and precision agricultural systems [92–100]. Engineered NPs have economical applications for enhanced plant growth, stimulate earlier plant germination and boosted plant production. Nanomaterials for agriculture use nanotechnology to advance the yield of plant products for nutritional food and feed, fuel, medicinal, and other purposes. Research in the area of nanoagriculture have suggested a wide gap in the information about the side effects of NPs on corn, rice, tomatoes, and other food crops [95,101,102]. A number of plants are able of uptake and accumulate nanomaterials and the research in this area showed that the uptake and build-up of engineered NPs depend on the type of plant, the chemical composition, size, concentration, surface structure, aggregation, and solubility of nanomaterials [103–105]. The interaction of plant cell with the engineered nanomaterials lead to the alteration of plant gene expression and associated biological pathways. The unique effects of nanomaterials on different plant species can differ significantly with plant growth stages, method, and duration of exposure [106].

Intensive investigations show that numerous engineered NPs are extremely toxic to a wide range of organisms such as, marine organisms, prokaryots, and animal cells *in vitro* (see Sect. 4.6.4 for more details). In addition, nanomaterials are generally very small that stays suspended for long time when released into the air [107–109]. Since NPs are very small, they follow air current NPs and are accumulated in all parts of the respiratory system of the plant [110–113]. Therefore, a particular concern is the capability of the NPs that are directly taken up by individual cells and cell nuclei, especially through the respiratory system.

In a recent study, Elmer and White investigated the enhancement in growth of tomatoes and eggplants using metallic oxide NPs. Spraying the leaves of tomato and eggplant with metallic oxide NPs could affect weight and production of the plants in disease-infected soils. They showed that metallic NPs such as CuO, MnO, and ZnO decreased disease rate compared to untreated controls [114].

Further research indicated that, further coating gives MIONPs large adsorption surface and biocompatible properties. For instance, in pumpkin (*Cucurbita pepo*), the presence of carbon-coated- Fe_3O_4 at certain concentrations reduces the quantity of chemicals released to the environment. Moreover, the effect of tetramethyl ammonium hydroxide-coated MIONPs on the growth of corn (*maize*) showed that the level of chlorophyll was amplified at low MIONPs concentration, whereas at higher concentrations it was inhibited [106].

Interestingly, Pariona et al. found that the engineered hematite and ferrihydrite NPs did not show toxicity or stress in maize seedlings. For example, the NP treatments enhanced the growth of maize and increased the chlorophyll content. While high hematite NPs (6 g L^{-1}) concentrations induced low inhibitory effects on germination and chlorophyll content, all the ferrihydrite treatments showed improvement in biological indicators. This is likely to be due to a large variety of products containing naturally occurring ferrihydrite NPs, which may work as iron source for the growth of the plants [115].

Rui et al. investigated the efficiency of MIONPs as a fertilizer to substitute traditional Fe fertilizers, which have several limitations. They investigated the unique effects of the MIONPs and a iron chelator (ethylenediaminetetraacetic acid-Fe; EDTA-Fe) on the development and growth of peanut (*Arachishypogaea*), a crop that is very sensitive to Fe insufficiency. The results showed that MIONPs increased height, biomass and root length of peanut plants. The Fe_2O_3 NPs stimulated the development of peanut by regulating plant hormones content and the activity of some antioxidant enzymes. They found that the concentration of Fe in peanut plants was higher than the control in the presence of MIONPs and EDTA-Fe. These findings demonstrate that Fe_2O_3 NPs can replace traditional Fe fertilizers in the farming of peanut plants [116].

MIONPs also find its application in increasing the fertility of soil. It has been reported that magnetic treatment of *Paenibaccilus* species increase their nitrogen-fixing ability and growth with a shorter generation time [117].

Yang et al. reported the different phytotoxicity of seven metal oxide NPs—nCeO2, nFe3O4, nSiO2, nTiO2, nAl2O3, nZnO, and nCuO—in maize and rice. They showed that seed germination of maize and rice was not affected by all the seven metal oxide NPs, while the root elongation of both maize and rice were significantly inhibited by nCuO and nZnO at 2000 mg L^{-1}. In addition, ZnO NPs showed greater toxicity to root elongation of maize and rice than ZnO MPs. They indicated that, this study provided a unified method to test the phytotoxicity of metal oxide NPs on crop plants [118].

Absorption of high amounts of metals by plants results in toxic effects that include decline in growth and abnormalities in cell division. Under this circumstance, excess metal NPs, work as enzymatic cofactor that are involved in making intermediate metabolites. Nevertheless, the reaction of plants to metal NPs differs with the nature of the metal, plant types, and the stage of growth [119,120].

At certain concentrations, MIONPs resulted in negative effect toward plant growth. For instance, the levels of "Chlorophyll a" were increased at low Fe_3O_4NPs concentra-

tions, though at higher concentrations it inhibited [121,122]. A slight inhibitory effect was noticed on the growth of the plantlets, which resulted in the formation of brown spots on the leaves at higher concentrations of MIONPs. Additionally, higher concentrations of MIONPs resulted in oxidative stress, which affected photosynthesis and caused a decrease in the rates of metabolic processes [123].

Bombin et al., reported that the charged MIONPs have inhibitory effects on the growth and reproduction in *A. thaliana*. They indicated that charged IONPs are transported via each tissue of the plant, so they were detected in root, leaf, flower and silique tissue. Positively charged Fe_2O_3 NPs showed substantial effects on root length and seedling in *A. thaliana* [124].

Both negatively and positively charged NPs revealed significant effects on pollen tube growth, seed production and pollen viability. These data indicate that MIONPs have a damaging effect on overall plant reproduction. In addition to that, the results showed that IONPs toxicity is greatly dependent on the concentration of the NPs [124].

Li et al. investigated the physiological effect of MIONPs on watermelon. They showed that a substantial quantity of Fe_2O_3 NPs dissolved in an aqueous medium might be taken up by watermelon tissue. Their findings demonstrated significant changes in the physiological factors including, activities of catalase, peroxidase, superoxide dismutase, root activity, and chlorophyll content. These results provide conclusive proof that plant uptake is a possible route for the transport of nanomaterials to the environment [125].

Organophosphorus insecticides are widely used to protect crops from harmful effects of insects but ultimately end up in water bodies and find a way to reach our bodies. Organophosphorus compounds are highly neurotoxic [126]. Maize acetylcholinesterase covalently attached onto Fe_3O_4/c-MWCNT modified gold electrode has been developed to detect the organophosphorus pesticide level as low as 0.1–10 nM in milk and water [127].

It is envisaged that in near future, MIONP-based catalysts will be available to increase the potency of pesticides and herbicides, letting lower doses to be employed in the field. An agricultural system called a Controlled Environment Agriculture (CEA) is widely used in the USA, Europe, and Japan, which efficiently utilizes technology for crop management. Plants are grown within a controlled environment so that agricultural practices can be optimized. CEA technology offers an excellent platform for the introduction of nanotechnology to agriculture. MIONPs and advanced nanotechnological devices tested under CEA can provide "scouting" capabilities that could tremendously improve the grower's ability to determine the best time to harvest the crop, the vitality of crop, and food security issues, such as microbial or chemical contamination.

4.5 Medical and Health

MIONPs find vast applications in the health and medical sectors. Medical use of MIONPs was reported by the Egyptian physician and philosopher Avicenna as far back as tenth century A.D. He used magnetite grain as an antidote for accidental swallowing of rust. MNPs could be used to increase contrast of magnetic resonance imaging (MRI). They can act as carrier for specific drug and gene therapy and also find their use in various processes like biosensing, bioseparation, immunotherapies. Although many NPs with specific molecules can be used to target metastasizing cells [128], MIONPs have additional advantage to release drug at a precise site by localized heat induced by magnetic field. Moreover, heat induced by localized magnetic field in the presence of magnetic beads can also be used to kill certain cancer cells as these cells are sensitive to temperatures greater than 41 °C [129,130]. It has been reported that many protein are deregulated in various cancers [131–133]. Drugs or inhibitors against a specific protein can be loaded on to MNPs and delivered at exact locations. MIONPs may also be used to detoxify the biological fluids; for example, magnetic beads coated with antibodies against epithelial surface antigens (ESA, clone VU-1D9) can be used to purify blood samples [134].

Tissue specific (adult) stem cells could be used to repair damaged or degenerated tissue by targeting them with MIONPs attached to various growth factors. This could lead to the differentiation of these cells with concomitant repair of the damaged tissue. This strategy could be used to treat and cure many degenerative ailments including diabetes and Alzheimer's and Parkinson's disease [135,136]. The blood–brain barrier severely limits permeability of various harmful toxins and bacteria in the blood stream from entering this vital organ thus protecting the brain from their harmful effects. However, this process also prevents many drugs from reaching the brain, creating a major problem in treating brain tumors and various neurological disorders such as Alzheimer's and Parkinson's disease, etc. NPs have potential to pass through blood-biological barriers. NPs loaded with anticancer drugs, such as loperamide and doxorubicin, could be used to deliver such drugs at therapeutic concentrations in the brain [137,138]. MIONPs coated with polycation, e.g., polyethylenimine could be used to transfect specific cells by the influence of an external magnetic field. This method of transfection called magnetofection could be used to transfect both viral and non-viral vectors. Magnetofection has been successfully used to transfect porcine kidney PK-15 cells with high efficiency [139].

Gene therapy is emerging as a valuable technique for the treatment or prevention of many diseases. In this technique, gene of a particular protein is delivered into a patient's cells as a drug for the treatment of the disease. Magnetofaction

provides a tool for the delivery of both viral and non-viral vectors [140]. One of the current challenges in gene therapy is the design of more advanced non-viral systems that could deliver gene for therapy with high efficiency. Increasing use of MIONPs that are able to circumvent these barriers are being exploited. There are increasing reports that IONPs have promising role in biosensing, because of their large surface to volume ratio, high surface reaction activity, and strong adsorption [141]. Glucose oxidase immobilized onto chitosan and nafion IONP-based glucose biosensors are proving highly sensitive and stable biosensors that can detect glucose in the range of 1.0–8.0 mM [142]. These sensors have good shelf life of about 8 weeks under refrigerated conditions and are proving very valuable tool for the management of diabetes [142,143]. Urease immobilized onto chitosan IONPs could be used for rapid and accurate measurement of urea in urine, serum, and blood samples [144].

4.6 Environmental Applications

Pollution-free environment is essential to human health; however, the world is facing environmental crisis that is increasing with time. Persistent organic pollutants, heavy metals, aquatic and soil pollutants are the major contributors toward the problem. MIONPs find wide applications in the field of wastewater treatment, as a part of a biosensor for the detection of environmental pollutants, dye degradation and adsorption, metal oxidation/reduction to render them harmless or removal through adsorption, and also in the degradation of phenolics, pesticides, petroleum hydrocarbons, and polycyclic aromatic hydrocarbons (PAH). The broad applications of MIONPs in waste treatment is due to large surface area, availability of complex chemistries and their facile recovery. Some key applications of MIONPs are discussed in the following sections.

4.6.1 Biosensors

Localized surface plasmonic resonance (LSPR) is widely used to monitor a broad range of analyte surface-binding interactions, including the adsorption of small molecules, ligand–receptor binding, protein adsorption on self-assembled monolayers, antibody–antigen binding, DNA and RNA hybridization, and protein–DNA interactions [145]. These sensors specifically identify low concentrations of environmental and biological substances usually from nL to μL range [146]. When samples are loaded on plain NPs for analysis, it usually lead to aggregation of NPs with the changes in the pH, ionic strength, and temperature. This problem is avoided by coating other molecules or nanostructures on iron oxide that protects them from aggregation.

4.6.2 Removal of Inorganic Pollutants

The concentrations of heavy metals have reached harmful levels throughout the world. Many methods have been developed for the effective detection and removal of these pollutants including the use of MIONPs. Physical sorption and ionic interactions between positively charged metal cations or negatively charged metal oxides and MIONP (or MIONPs with additional coatings such as silica, alumina and various polymers) are the main processes involved in the removal of metals from solutions. IONPs have been effectively used to remove lead (Pb^{2+}) and mercury (Hg^{2+}) [147], arsenic (As) [148], copper (Cu^{2+}) [149] etc. For example, a novel reusable MIONP coated with chitosan and cross-linked to glyoxal (Fe_3O_4/chitosan/glyoxal) has recently been used to adsorb 80–90% of toxic chromium (VI) from water [150]. At pH 4, Cr (VI) exists predominantly as $HCrO_4^-$ and interacts electrostatically with the positively charged NH_3^+ groups on chitosan. After collecting the MIONP–metal complexes by the application of magnetic field, an increase in pH deprotonates the positively charged amino groups to NH_2 thereby releasing chromium ions allowing the MIONPs to be reused [150]. Similarly, highly toxic cationic metals such as Cd^{2+}, Pb^{2+}, Ni^{2+} and Cu^{2+} have been efficiently removed by using 3-aminopropyl triethoxysilane (APTES)-coated MIONPs that were further modified with acrylic acid moieties. The adsorption efficiency increased with an increase in pH due to the deprotonation of carboxylic acid groups and the MIONPs were separated by the application of magnetic field. The metal ions were released by lowering the pH to 4 thereby regenerating MIONPs to be reused again [151]. Mesoporous Fe_3O_4 secondary nanostructures (MFSNs) have also been reported for the removal of As, Cd, and Cu from waste water [152].

4.6.3 Removal of Organic Pollutants

Surface modified magnetite nanoparticles with ferrous oxalate reducing agent were recently used to degrade azo dyes (Reactive Black and Reactive Yellow) in the presence of hydrogen peroxide [153]. The degradation follows Fenton's reaction mechanism where H_2O_2 is reduced by a metal reducing agent such as Fe(II) and in the process generates hydroxyl free radicals with concomitant degradation of organic pollutants by breaking covalent bonds. Although a very high degree of degradation of dyes ($> 99\%$) was achieved, however, the amount of catalyst used ($10\,g\,L^{-1}$) was high and the duration of degradation was long (240 min). Generally, in the presence of H_2O_2, azo dyes are degraded much faster [154].

A mixture of three textile azo dyes (Basic Blue-3, Basic Red 46 and Malachite Green) was degraded via Fenton reaction using modified natural magnetite nanoparticles (NMN)

prepared by a green glow discharge plasma (GDP) technology. GC–MS was used to show the degradation of dyes to smaller molecular weight products [155,156]. Similarly, removal of dyes from simulated sewage water was achieved by a 3D flower-shaped assembly of iron oxide nanosheets. These nanostructures were synthesized by the decomposition of various iron alkoxide precursors using heat treatment. These nanostructures acted as a highly effective sorbent for the fast removal of organic dyes such as Reactive Orange, Reactive Yellow and Bismarck Brown [157].

The synthesis of magnetic Fe_3O_4/NPC nanoporous carbon using metal oxide framwork-5 (MOF-5) with very high surface area and strong magnetic strength has recently been reported [158]. The behavior of MIONPs were tested by its adsorption capacity for the removal of methylene blue from the aqueous solution. The results showed that the synthesized material had a high adsorption capacity and fast adsorption rate. The adsorbent can be easily recovered with ethanol washing, and its susceptibility to an applied magnetic field. This material can be used for the effective removal of organic dyes from wastewater.

The magnetic cyclodextrin–graphene oxide nanocomposites (Fe_3O_4/CD/GO) were used to remove malachite green dye in a simple and effective manner [159]. The authors reported highly efficient removal of dye with concomitant high adsorption capacity. However, concentration of dye was measured by colorimetric method, which may be biased at different pHs, whereas quantification based on separation by HPLC at neutral pH may have been more accurate.

The encapsulated and functionalized Fe_3O_4 nanoparticles with silica and amino groups were immobilized on *Corynebacterium glutamicum* [160]. The magnetic particle-coated bacteria were used to degrade phenol successfully with concomitant recycling. However, the growth of bacterium was slow, and the duration of degradation was very long. Moreover, phenol degradation and adsorption was reduced in subsequent cycles compared to the original particles. Furthermore, IONPs can also efficiently remove organic wastes like polycyclic aromatic hydrocarbons (PAHs) and halogenated organic compounds (HOC) [161]. The PAHs and HOC were oxidized with concomitant degradation via a photocatalytical reaction. It is noteworthy that recently magnetic nanoparticle adsorbents with silica mesoporous layer that have surfactant micelles within it were used to achieve simultaneous, sustainable, rapid, efficient, and cost-effective removal of PAHs [1 mg L^{-1}] and metal contaminants [1 mg L^{-1}] [162].

Oil spill is a serious environmental issue that damages the aquatic life and severely disturbs the ecological balance. The current technology for the remediation of oil is inefficient and costly. Recently, iron-based magnetic nanoparticles that were capped by sulfonated asphaltene were used to collect a heavy crude oil spill without spreading it in water by applying an external magnetic field. Compared with currently available procedures, the process based on MIONPs with a hydrophobic linker achieved exceptional oil spill mopping efficiency (removal of 22.5 g of the crude oil from the sea water surface per gram nanomaterial) and a significant reduction in cost (US$ 2 per 1 kg nanomaterial). Based on the 95% yield of nanomaterial, the total cost for cleaning 1 barrel of crude oil was only 12 US$ [163].

4.6.4 Bio-indicators for the Assessment of MIONPs Toxicity

Although magnetic nanoparticles have been successfully exploited for numerous applications including environmental remediation, however, potential risks related to their release into the aquatic environment should be carefully assessed. The ecological and toxic effects of magnetic nanoparticle on aquatic life were assessed by monitoring early life stages of zebrafish (*Danio rerio*) [164]. It was observed that MIONPs (10 mg L^{-1}) caused developmental abnormalities in embryos including hatching delay, mortality, and malfunction. Where zebrafish was used as biomarker indicator for magnetic nanoparticle's toxicity toward animals, *Chlorella vulgaris* cells were tested for toxic effects of MIONPs against plants [165]. The algal cell when exposed to cobalt, zinc composite nanoparticles, showed reduced photosynthesis and induction of oxidative stress as well as inhibiting the cell division rate. Both organisms (fish and microalgae) can be used as key biomarker indicators for the assessment of nanoparticles toxicity.

5 Conclusion and Future Direction

In conclusion, smaller particle size, large surface area, and control of morphology are the major factors, which allow researchers to utilize MIONPs for various real and potential applications in fields as diverse as catalysis, energy harvesting, agriculture, environmental and medical sectors. MIONPs have been explored for the remediation of water and their magnetic properties enable them to be used for MRI and other related applications. In pristine form, MIONPs may show susceptibility toward corrosion, which limit their use and recovery during and after the reaction. In addition to these, agglomeration can also limit their effectiveness. In order to overcome these problems, researchers have introduced various functionalities via doping, mixing and other physiochemical methods to make them suitable for various applications with improved properties.

Although, MIONPs display various unique characteristics, which endow them with numerous benefits and present opportunities in various applications as discussed above. However, further ground-breaking research is needed regarding improvement in the synthetic techniques to create

MIONPs of controlled shape and size. The biggest challenge is agglomeration at nanoscale level, and therefore, special techniques are needed to be developed to minimize this problem in order to increase its viability for various applications. Another challenge is the susceptibility of MIONPs toward corrosion under wet conditions, which can affect its stability in addition to other key features. Toxicity caused by MIONPs is another challenge as it can arise during the processing of MIONPs or by its usage in the post production applications. There is a need to develop more suitable techniques that can selectively confer MIONPs with improved magnetic properties. Importantly, the exact mechanism (nucleation and growth) of formation of MIONPs of various morphologies needs to be understood. Moreover, introduction of certain organic and inorganic functionalities could also improve the corrosion resistance of MIONPs. Finally, the synthetic precursors of MIONPs could be chosen from non-toxic and biodegradable materials under controlled reaction conditions. MIONPs are cost-effective materials that have a bright future in numerous technological applications including energy harvesting devices and systems.

References

1. Mansha, M.; Qurashi, A.; Ullah, N.; Bakare, F.O.; Khan, I.; Yamani, Z.H.: Synthesis of In_2O_3/graphene heterostructure and their hydrogen gas sensing properties. Ceram. Int. **42**, 11490–11495 (2016). doi:10.1016/j.ceramint.2016.04.035
2. ullah, H.; Khan, I.; Yamani, Z.H.; Qurashi, A.: Sonochemical-driven ultrafast facile synthesis of SnO_2 nanoparticles: growth mechanism structural electrical and hydrogen gas sensing properties. Ultrason. Sonochem. **34**, 484–490 (2017). doi:10.1016/j.ultsonch.2016.06.025
3. Qurashi, A.; Alhaffar, M.; Yamani, Z.H.: Hierarchical ZnO/zeolite nanostructures: synthesis, growth mechanism and hydrogen detection. RSC Adv. **5**, 22570–22577 (2015). doi:10.1039/C4RA15497E
4. Qurashi, A.; Rather, J.A.; De Wael, K.; Merzougui, B.; Tabet, N.; Faiz, M.: Rapid microwave synthesis of high aspect-ratio ZnO nanotetrapods for swift bisphenol A detection. Analyst **138**, 4764 (2013). doi:10.1039/c3an00336a
5. Ahsanulhaq, Q.; Kim, J.H.; Hahn, Y.B.: Immobilization of angiotensin II and bovine serum albumin on strip-patterned ZnO nanorod arrays. J. Nanosci. Nanotechnol. **10**, 4159–4165 (2010). doi:10.1166/jnn.2010.2404
6. Saeed, K.; Khan, I.: Preparation and properties of single-walled carbon nanotubes/poly(butylene terephthalate) nanocomposites. Iran. Polym. J. **23**, 53–58 (2014). doi:10.1007/s13726-013-0199-2
7. Miller, M.M.; Prinz, G.A.; Cheng, S.-F.; Bounnak, S.: Detection of a micron-sized magnetic sphere using a ring-shaped anisotropic magnetoresistance-based sensor: a model for a magnetoresistance-based biosensor. Appl. Phys. Lett. **81**, 2211–2213 (2002). doi:10.1063/1.1507832
8. Jain, T.K.; Morales, M.A.; Sahoo, S.K.; Leslie-Pelecky, D.L.; Labhasetwar, V.: Iron oxide nanoparticles for sustained delivery of anticancer agents. Mol. Pharm. **2**(3), 194–205 (2005). doi:10.1021/MP0500014
9. Modo, M.M.; Bulte, J.W. (eds.): Molecular and Cellular MR Imaging. CRC Press, Boca Raton (2007)
10. Shen, Z.; Wu, A.; Chen, X.: Iron oxide nanoparticle based contrast agents for magnetic resonance imaging. Mol. Pharm. **14**, 1352–1364 (2017). doi:10.1021/acs.molpharmaceut.6b00839
11. Chiolerio, A.; Chiodoni, A.; Allia, P.; Martino, P.: Magnetite and other Fe-oxide nanoparticles. In: Handbook of Nanomaterials Properties. pp. 213–246. Springer, Berlin (2014)
12. Charles, S.W.; Popplewell, J.: Properties and applications of magnetic liquids. Endeavour **6**, 153–161 (1982). doi:10.1016/0160-9327(82)90070-9
13. Atashin, H.; Malakooti, R.: Magnetic iron oxide nanoparticles embedded in SBA-15 silica wall as a green and recoverable catalyst for the oxidation of alcohols and sulfides. J. Saudi Chem. Soc. **21**, S17–S24 (2017). doi:10.1016/j.jscs.2013.09.007
14. Arora, A.K.; Sharma, M.; Kumari, R.; Jaswal, V.S.; Kumar, P.: Synthesis, characterization, and magnetic studies of α-Fe_2O_3 nanoparticles. J. Nanotechnol. **2014**, 1–7 (2014). doi:10.1155/2014/474909
15. Vengsarkar, P.S.; Xu, R.; Roberts, C.B.: Deposition of iron oxide nanoparticles onto an oxidic support using a novel gas-expanded liquid process to produce functional Fischer–Tropsch synthesis catalysts. Ind. Eng. Chem. Res. **54**, 11814–11824 (2015). doi:10.1021/acs.iecr.5b03123
16. Rioult, M.; Stanescu, D.; Fonda, E.; Barbier, A.; Magnan, H.: Oxygen vacancies engineering of iron oxides films for solar water splitting. J. Phys. Chem. C **120**, 7482–7490 (2016). doi:10.1021/acs.jpcc.6b00552
17. Dias, P.; Vilanova, A.; Lopes, T.; Andrade, L.; Mendes, A.: Extremely stable bare hematite photoanode for solar water splitting. Nano Energy **23**, 70–79 (2016). doi:10.1016/j.nanoen.2016.03.008
18. Wu, W.; He, Q.; Jiang, C.: Magnetic iron oxide nanoparticles: synthesis and surface functionalization strategies. Nanoscale Res. Lett. **3**, 397–415 (2008). doi:10.1007/s11671-008-9174-9
19. Ali, A.; Zafar, H.; Zia, M.; Ul Haq, I.; Phull, A.R.; Ali, J.S.; Hussain, A.: Synthesis, characterization, applications, and challenges of iron oxide nanoparticles. Nanotechnol. Sci. Appl. **9**, 49–67 (2016). doi:10.2147/NSA.S99986
20. Wu, W.; Xiao, X.; Zhang, S.; Zhou, J.; Fan, L.; Ren, F.; Jiang, C.: Large-scale and controlled synthesis of iron oxide magnetic short nanotubes: shape evolution, growth mechanism, and magnetic properties. J. Phys. Chem. C **114**, 16092–16103 (2010). doi:10.1021/jp1010154
21. Tartaj, P.; Morales, M.P.; Gonzalez-Carreño, T.; Veintemillas-Verdaguer, S.; Serna, C.J.: The iron oxides strike back: from biomedical applications to energy storage devices and photoelectrochemical water splitting. Adv. Mater. **23**, 5243–5249 (2011). doi:10.1002/adma.201101368
22. Qurashi, A.; Zhong, Z.; Alam, M.W.: Synthesis and photocatalytic properties of α-Fe_2O_3 nanoellipsoids. Solid State Sci. **12**, 1516–1519 (2010). doi:10.1016/j.solidstatesciences.2010.05.001
23. Wu, W.; Wu, Z.; Yu, T.; Jiang, C.; Kim, W.-S.: Recent progress on magnetic iron oxide nanoparticles: synthesis, surface functional strategies and biomedical applications. Sci. Technol. Adv. Mater. **16**, 23501 (2015). doi:10.1088/1468-6996/16/2/023501
24. Chirita, M.; Grozescu, I.: Fe_2O_3-nanoparticles, physical properties and their photochemical and photoelectrochemical applications. Chem. Bull. Polit. Univ. Timsisoara **54**, 1–8 (2009)
25. Ding, Y.; Morber, J.R.; Snyder, R.L.; Wang, Z.L.: Nanowire structural evolution from Fe_3O_4 to ε-Fe_2O_3. Adv. Funct. Mater. **17**, 1172–1178 (2007). doi:10.1002/adfm.200601024
26. Chung, Y.; Lim, S.K.; Kim, C.K.; Kim, Y.-H.; Yoon, C.S.: Synthesis of γ-Fe_2O_3 nanoparticles embedded in polyimide. J. Magn. Magn. Mater. **272–276**, E1167–E1168 (2004). doi:10.1016/j.jmmm.2003.12.217

27. Li, F.; Luo, S.; Sun, Z.; Bao, X.; Fan, L.-S.: Role of metal oxide support in redox reactions of iron oxide for chemical looping applications: experiments and density functional theory calculations. Energy Environ. Sci. **4**, 3661 (2011). doi:10.1039/c1ee01325d
28. Darken, L.S.; Gurry, R.W.: The system iron–oxygen. I. The Wüstite field and related equilibria. J. Am. Chem. Soc. **67**, 1398–1412 (1945). doi:10.1021/ja01224a050
29. Teja, A.S.; Koh, P.-Y.: Synthesis, properties, and applications of magnetic iron oxide nanoparticles. Prog. Cryst. Growth Charact. Mater. **55**, 22–45 (2009). doi:10.1016/j.pcrysgrow.2008.08.003
30. Yamaura, M.; Camilo, R.; Sampaio, L.; Macêdo, M.; Nakamura, M.; Toma, H.: Preparation and characterization of (3-aminopropyl)triethoxysilane-coated magnetite nanoparticles. J. Magn. Magn. Mater. **279**, 210–217 (2004). doi:10.1016/j.jmmm.2004.01.094
31. Ceylan, A.; Baker, C.C.; Hasanain, S.K.; Ismat Shah, S.: Effect of particle size on the magnetic properties of core–shell structured nanoparticles. J. Appl. Phys. **100**, 34301 (2006). doi:10.1063/1.2219691
32. Levy, M.; Quarta, A.; Espinosa, A.; Figuerola, A.; Wilhelm, C.; García-Hernández, M.; Genovese, A.; Falqui, A.; Alloyeau, D.; Buonsanti, R.; Cozzoli, P.D.; García, M.A.; Gazeau, F.; Pellegrino, T.: Correlating magneto-structural properties to hyperthermia performance of highly monodisperse iron oxide nanoparticles prepared by a seeded-growth route. Chem. Mater. **23**, 4170–4180 (2011). doi:10.1021/cm201078f
33. Guardia, P.; Labarta, A.; Batlle, X.: Tuning the size, the shape, and the magnetic properties of iron oxide nanoparticles. J. Phys. Chem. C **115**, 390–396 (2011). doi:10.1021/jp1084982
34. Bharathi, S.; Nataraj, D.; Seetha, M.; Mangalaraj, D.; Ponpandian, N.; Masuda, Y.; Senthil, K.; Yong, K.: Controlled growth of single-crystalline, nanostructured dendrites and snowflakes of α-Fe_2O_3: influence of the surfactant on the morphology and investigation of morphology dependent magnetic properties. CrystEngComm **12**, 373–382 (2010). doi:10.1039/B910550F
35. Wang, Y.; Xia, Y.: Bottom-up and top-down approaches to the synthesis of monodispersed spherical colloids of low melting-point metals. Nano Lett. **4**, 2047–2050 (2004). doi:10.1021/nl048689j
36. Liu, J.; Wu, Z.; Tian, Q.; Wu, W.; Xiao, X.: Shape-controlled iron oxide nanocrystals: synthesis, magnetic properties and energy conversion applications. CrystEngComm **18**, 6303–6326 (2016). doi:10.1039/C6CE01307D
37. Riasat, R.; Nie, G.: Synthesis and characterization of non-toxic hollow iron oxide (α-Fe_2O_3) nanoparticles using a simple hydrothermal strategy. J. Nanomater. **2016**, 1–7 (2016). doi:10.1155/2016/1920475
38. Khalil, M.I.: Co-precipitation in aqueous solution synthesis of magnetite nanoparticles using iron(III) salts as precursors. Arab. J. Chem. **8**, 279–284 (2015). doi:10.1016/j.arabjc.2015.02.008
39. Wu, S.; Sun, A.; Zhai, F.; Wang, J.; Xu, W.; Zhang, Q.; Volinsky, A.A.: Fe_3O_4 magnetic nanoparticles synthesis from tailings by ultrasonic chemical co-precipitation. Mater. Lett. **65**, 1882–1884 (2011). doi:10.1016/j.matlet.2011.03.065
40. Pandey, S.; Mishra, S.B.: Sol–gel derived organic-inorganic hybrid materials: synthesis, characterizations and applications. J. Sol–Gel Sci. Technol. **59**, 73–94 (2011). doi:10.1007/s10971-011-2465-0
41. Florini, N.; Barrera, G.; Tiberto, P.; Allia, P.; Bondioli, F.: Non-aqueous sol–gel synthesis of magnetic iron oxides nanocrystals. J. Am. Ceram. Soc. (2013). doi:10.1111/jace.12469
42. Lemine, O.M.; Omri, K.; Zhang, B.; El Mir, L.; Sajieddine, M.; Alyamani, A.; Bououdina, M.: Sol–gel synthesis of 8nm magnetite (Fe_3O_4) nanoparticles and their magnetic properties. Superlattices Microstruct. **52**, 793–799 (2012). doi:10.1016/j.spmi.2012.07.009
43. Unni, M.; Uhl, A.M.; Savliwala, S.; Savitzky, B.H.; Dhavalikar, R.; Garraud, N.; Arnold, D.P.; Kourkoutis, L.F.; Andrew, J.S.; Rinaldi, C.: Thermal decomposition synthesis of iron oxide nanoparticles with diminished magnetic dead layer by controlled addition of oxygen. ACS Nano **11**, 2284–2303 (2017). doi:10.1021/acsnano.7b00609
44. Kozakova, Z.; Kuritka, I.; Kazantseva, N.E.; Babayan, V.; Pastorek, M.; Machovsky, M.; Bazant, P.; Saha, P.: The formation mechanism of iron oxide nanoparticles within the microwave-assisted solvothermal synthesis and its correlation with the structural and magnetic properties. Dalt. Trans. **44**, 21099–21108 (2015). doi:10.1039/C5DT03518J
45. Khan, I.; Ali, S.; Mansha, M.; Qurashi, A.: Sonochemical assisted hydrothermal synthesis of pseudo-flower shaped Bismuth vanadate ($BiVO_4$) and their solar-driven water splitting application. Ultrason. Sonochem. **36**, 386–392 (2017). doi:10.1016/j.ultsonch.2016.12.014
46. Zhuang, L.; Zhang, W.; Zhao, Y.; Shen, H.; Lin, H.; Liang, J.: Preparation and characterization of Fe_3O_4 particles with novel nanosheets morphology and magnetochromatic property by a modified solvothermal method. Sci. Rep. **5**, 9320 (2015). doi:10.1038/srep09320
47. Khan, I.; Abdalla, A.; Qurashi, A.: Synthesis of hierarchical WO_3 and Bi_2O_3/WO_3 nanocomposite for solar-driven water splitting applications. Int. J. Hydrogen Energy **42**, 3431–3439 (2017). doi:10.1016/j.ijhydene.2016.11.105
48. Mansha, M.; Khan, I.; Ullah, N.; Qurashi, A.: Synthesis, characterization and visible-light-driven photoelectrochemical hydrogen evolution reaction of carbazole-containing conjugated polymers. Int. J. Hydrogen Energy. (2017). doi:10.1016/j.ijhydene.2017.02.053
49. Khan, I.; Ibrahim, A.A.M.; Sohail, M.; Qurashi, A.: Sonochemical assisted synthesis of RGO/ZnO nanowire arrays for photoelectrochemical water splitting. Ultrason. Sonochem. **37**, 669–675 (2017). doi:10.1016/j.ultsonch.2017.02.029
50. Iqbal, N.; Khan, I.; Yamani, Z.H.; Qurashi, A.: Sonochemical assisted solvothermal synthesis of gallium oxynitride nanosheets and their solar-driven photoelectrochemical water-splitting applications. Sci. Rep. **6**, 32319 (2016). doi:10.1038/srep32319
51. Iqbal, N.; Khan, I.; Yamani, Z.H.A.; Qurashi, A.: A facile one-step strategy for in-situ fabrication of WO_3-$BiVO_4$ nanoarrays for solar-driven photoelectrochemical water splitting applications. Sol. Energy **144**, 604–611 (2017). doi:10.1016/j.solener.2017.01.057
52. Mansha, M.; Khan, I.; Ullah, N.; Qurashi, A.; Sohail, M.: Visible-light driven photocatalytic oxygen evolution reaction from new poly(phenylene cyanovinylenes). Dye Pigment. (2017). doi:10.1016/j.dyepig.2017.04.028
53. Avasare, V.; Zhang, Z.; Avasare, D.; Khan, I.; Qurashi, A.: Room-temperature synthesis of TiO_2 nanospheres and their solar driven photoelectrochemical hydrogen production. Int. J. Energy Res. **39**, 1714–1719 (2015). doi:10.1002/er.3372
54. Sivula, K.; Le Formal, F.; Grätzel, M.; Le Formal, F.; Grätzel, M.: Solar water splitting: progress using hematite (α-Fe_2O_3) photoelectrodes. ChemSusChem **4**, 432–449 (2011). doi:10.1002/cssc.201000416
55. Charvin, P.; Abanades, S.; Flamant, G.; Lemort, F.: Two-step water splitting thermochemical cycle based on iron oxide redox pair for solar hydrogen production. Energy **32**, 1124–1133 (2007). doi:10.1016/j.energy.2006.07.023
56. Gokon, N.; Murayama, H.; Umeda, J.; Hatamachi, T.; Kodama, T.: Monoclinic zirconia-supported Fe_3O_4 for the two-step water-splitting thermochemical cycle at high thermal reduction temperatures of 1400–1600°C. Int. J. Hydrogen Energy **34**, 1208–1217 (2009). doi:10.1016/j.ijhydene.2008.12.007

57. Hagfeldt, A.; Boschloo, G.; Sun, L.; Kloo, L.; Pettersson, H.: Dye-sensitized solar cells. Chem. Rev. **110**, 6595–6663 (2010). doi:10.1021/cr900356p
58. Grätzel, M.; Bach, U.; Lupo, D.; Comte, P.; Moser, J.E.; Weissörtel, F.; Salbeck, J.; Spreitzer, H.: Solid-state dye-sensitized mesoporous TiO_2 solar cells with high photon-to-electron conversion efficiencies. Nature **395**, 583–585 (1998). doi:10.1038/26936
59. Agarwala, S.; Lim, Z.H.; Nicholson, E.; Ho, G.W.: Probing the morphology-device relation of Fe_2O_3 nanostructures towards photovoltaic and sensing applications. Nanoscale **4**, 194–205 (2012). doi:10.1039/C1NR10856E
60. Manikandan, A.; Saravanan, A.; Antony, S.A.; Bououdina, M.: One-pot low temperature synthesis and characterization studies of nanocrystalline α-Fe_2O_3 based dye sensitized solar cells. J. Nanosci. Nanotechnol. **15**, 4358–4366 (2015). doi:10.1166/jnn.2015.9804
61. Wang, W.; Pan, X.; Liu, W.; Zhang, B.; Chen, H.; Fang, X.; Yao, J.; Dai, S.; Comte, P.; Pechy, P.; Gratzel, M.: $FeSe_2$ films with controllable morphologies as efficient counter electrodes for dye-sensitized solar cells. Chem. Commun. **50**, 2618 (2014). doi:10.1039/c3cc49175g
62. Wang, L.; Shi, Y.; Zhang, H.; Bai, X.; Wang, Y.; Ma, T.: Iron oxide nanostructures as highly efficient heterogeneous catalysts for mesoscopic photovoltaics. J. Mater. Chem. A. **2**, 15279 (2014). doi:10.1039/C4TA03727H
63. Albo, J.; Alvarez-Guerra, M.; Castaño, P.; Irabien, A.: Towards the electrochemical conversion of carbon dioxide into methanol. Green Chem. **17**, 2304–2324 (2015). doi:10.1039/C4GC02453B
64. Graves, C.; Ebbesen, S.D.; Mogensen, M.; Lackner, K.S.: Sustainable hydrocarbon fuels by recycling CO_2 and H_2O with renewable or nuclear energy. Renew. Sustain. Energy Rev. **15**, 1–23 (2011). doi:10.1016/j.rser.2010.07.014
65. Abanades, S.; Villafan-Vidales, I.: CO_2 valorisation based on Fe_3O_4/FeO thermochemical redox reactions using concentrated solar energy. Int. J. Energy Res. **37**, 598–608 (2013). doi:10.1002/er.1953
66. Fan, G.; Luo, S.; Wu, Q.; Fang, T.; Li, J.; Song, G.; Hyeon, T.: $ZnBr_2$ supported on silica-coated magnetic nanoparticles of Fe_3O_4 for conversion of CO_2 to diphenyl carbonate. RSC Adv. **5**, 56478–56485 (2015). doi:10.1039/C5RA07431B
67. Wei, S.; Wang, Q.; Zhu, J.; Sun, L.; Lin, H.; Guo, Z.: Multifunctional composite core-shell nanoparticles. Nanoscale **3**, 4474–4502 (2011). doi:10.1039/C1NR11000D
68. Yoon, T.-J.; Lee, W.; Oh, Y.-S.; Lee, J.-K.: Magnetic nanoparticles as a catalyst vehicle for simple and easy recycling. New J. Chem. **27**, 227–229 (2003). doi:10.1039/B209391J
69. Zolfigola, M.A.; Nasrabadia, R.A.; Bagherya, S.; Khakyzadehb, V.; Azizian, S.: Applications of a novel nano magnetic catalyst in the synthesis of1,8-dioxo-octahydroxanthene and dihydropyrano[2,3-c] pyrazolederivatives. J. Mol. Catal. A Chem. **418–419**, 54–67 (2016)
70. Zolfigol, M.A.; Azadbakht, T.; Khakyzadeh, V.; Nejatyamid, R.; Perrinb, D.M.: C(*sp*2)–C(*sp*2) cross coupling reactions catalyzed by an active and highly stable magnetically separable Pd-nanocatalyst in aqueous media. RSC Adv. **4**, 40036–40042 (2014)
71. Baharfar, R.; Mohajer, M.: Synthesis and characterization of immobilized lipase on Fe_3O_4 nanoparticles as nano biocatalyst for the synthesis of benzothiazepine and spirobenzothiazine chroman derivatives. Catal. Lett. **146**, 1729–1742 (2016)
72. Meshkani, F.; Rezaei, M.: Preparation of mesoporous nanocrystalline iron based catalysts for high temperature water gas shift reaction: effect of preparation factors. Chem. Eng. J. **260**, 107–116 (2015)
73. Dehghani, F.; Sardarian, A.R.; Esmaeilpour, M.: Salen complex of Cu(II) supported on superparamagnetic Fe_3O_4@SiO_2 nanoparticles: an efficient and recyclable catalyst for synthesis of 1-and 5-substituted 1h-tetrazoles. J. Org. Chem. **743**, 87–96 (2013)
74. Esmaeilpour, M.; Sardarian, A.R.; Javidi, J.: Schiff base complex of metal ions supported on superparamagnetic Fe_3O_4@SiO_2 nanoparticles: an efficient, selective and recyclable catalyst for synthesis of 1,1-diacetates from aldehydes under solvent-free conditions. Appl. Catal. A **445–446**, 359–367 (2012)
75. Naeimi, H.; Nazifi, Z.A.: Highly efficient nano-Fe_3O_4 encapsulated-silica particles bearing sulfonic acid groups as a solid acid catalyst for synthesis of 1,8-dioxo-octahydroxanthene derivatives. J. Nanopart. Res. **15**, 2026 (2013)
76. Ucoski, G.M.; Nunes, F.S.; DeFreitas-Silva, G.; Idemori, Y.M.; Nakagaki, S.: Metalloporphyrins immobilized on silica-coated Fe_3O_4 nanoparticles: magnetically recoverable catalysts for the oxidation of organic substrates. Appl. Catal. A **459**, 121–130 (2013)
77. Rayati, S.; Abdolalian, P.: Heterogenization of a molybdenum schiff base complex as a magnetic nanocatalyst: an eco-friendly, efficient, selective and recyclable nanocatalyst for the oxidation of alkenes. C. R. Chim. **16**, 814–820 (2013)
78. Rhodes, C.; Hutchings, G.J.: Studies of the role of the copper promoter in the iron oxide/chromia high temperature water gas shift catalyst. Phys. Chem. Chem. Phys. **5**, 2719 (2003)
79. Gawade, P.; Mirkelamoglu, B.; Tan, B.; Ozkan, U.S.: Cr-free Fe-based water-gas shift catalysts prepared through propylene oxide-assisted sol–gel technique. J. Mol. Catal. A Chem. **321**, 61–70 (2010)
80. Yan, Q.; Street, J.; Yu, F.: Synthesis of carbon-encapsulated iron nanoparticles from wood derived sugars by hydrothermal carbonization (HTC) and their application to convert bio-syngas into liquid hydrocarbons. Biomass Bioenergy **83**, 85–95 (2015)
81. Galvis, H.M.T.; Bitter, J.H.; Khare, C.B.; Ruitenbeek, M.; Dugulan, A.I.; De Jong, K.P.: Supported iron nanoparticles as catalysts for sustainable production of lower olefins. Science **335**, 835 (2012)
82. Pour, A.N.; Taghipoor, S.; Shekarriz, M.; Shahri, S.M.; Zamani, Y.: Fischere–Tropsch synthesis with Fe/Cu/La/SiO_2 nanostructured catalyst. J. Nanosci. Nanotechnol. **9**, 4425–4433 (2009)
83. Li, X.; Lei, Y.; Li, X.; Song, S.; Wang, C.; Zhang, H.: Morphology-controlled synthesis of a-Fe_2O_3 nanostructures with magnetic property and excellent electrocatalytic activity for H2O2. Solid StateSci. **13**, 2129–2136 (2011)
84. Rafiee, E.; Joshaghania, M.; Abadi, P.G.S.: Shape-dependent catalytic activity of Fe_3O_4 nanostructures under the influence of an external magnetic field for multicomponent reactions in aqueous media. R. Soc. Chem. Adv. **5**, 74091–74101 (2015)
85. Byrne, S.J.; Corr, S.A.; Gun'ko, Y.K.; Kelly, J.M.; Brougham, D.F.; Ghosh, S.: Magnetic nanoparticle assemblies on denatured DNA show unusual magnetic relaxivity and potential applications for MRI. Chem. Commun. **22**, 2560–2561 (2004)
86. Nasongkla, N.; Bey, E.; Ren, J.; Ai, H.; Khemtong, C.; Guthi, J.S.; Chin, S.-F.; Sherry, A.D.; Boothman, D.A.; Gao, J.: Multifunctional polymeric micelles as cancer-targeted, MRI-ultrasensitive drug delivery systems. Nano Lett. **6**, 2427–2430 (2006)
87. Figuerola, A.; Di Corato, R.; Manna, L.; Pellegrino, T.: From iron oxide nanoparticles towards advanced iron-based inorganic materials designed for biomedical applications. Pharmacol. Res. **62**(2), 126–143 (2010)
88. Dobson, J.: Magnetic nanoparticles for drug delivery. Drug Dev. Res. **67**, 55–60 (2006)
89. Ribeiro, G.A.P.: As propriedades magnéticas da matéria: um primeiro contato. Revista Brasileira de Ensino de Física **22**(3), 299–305 (2000)

90. Salata, O.V.: Applications of nanoparticles in biology and medicine. J. Nanobiotechnol. **2**(1), 3 (2004)
91. Freitas, J.C.D.; Branco, R.M.; Lisboa, I.G.O.; Da Costa, T.P.; Campos, M.G.N.; Júnior, M.J.; Marques, R.F.C.: Magnetic nanoparticles obtained by homogeneous coprecipitation sonochemically assisted. Mater. Res. **18**(Sup 2), 220–224 (2015)
92. Musee, N.: Nanowastes and the environment: potential new waste management paradigm. Environ. Int. **37**(1), 112–128 (2011)
93. Hansen, S.F; Baun, A; Michelson, E.S.; Kamper, A; Borling, P; Stuer-Lauridsen, F: Nanomaterials in consumer products. Nanomater. Risks Benefits 359–367 (2009)
94. Bandyopadhyay, S.; Peralta-Videa, J.R.; Gardea-Torresdey, J.L.: Advanced analytical techniques for the measurement of nanomaterials in food and agricultural samples: a review. Environ. Eng. Sci. **30**(3), 118–125 (2013)
95. Nadiminti, P.P.; Dong, Y.D.; Sayer, C.; Hay, P.; Rookest, J.E.; Boyd, B.J.; Cahill, D.M.: Nanostructured liquid crystalline particles as an alternative delivery vehicle for plant agrochemicals. ACS Appl. Mater. Interfaces **5**(5), 1818–1826 (2013)
96. Delgado-Ramos, G.C.: Nanotechnology in Mexico: global trends and national implications for policy and regulatory issues. Technol. Soc. **37**(1), 4–15 (2014)
97. Safari, J.; Zarnegar, Z.: Advanced drug delivery systems: nanotechnology of health design: a review. J. Saudi Chem. Soc. **18**(2), 85–99 (2014)
98. Neto, O.P.V.: Intelligent computational nanotechnology: the role of computational intelligence in the development of nanoscience and nanotechnology. J. Comput. Theor. Nanosci. **11**(4), 928–944 (2014)
99. Dutschk, V.; Karapantsios, T.; Liggieri, L.; McMillan, N.; Miller, R.; Starov, V.M.: Smart and green interfaces: from single bubbles/drops to industrial environmental and biomedical applications. Adv. Colloid Interface Sci. **209**, 109–126 (2014)
100. Al-Halafi, A.M.: Nanocarriers of nanotechnology in retinal diseases. Saudi J. Ophthalmol. **28**(4), 304–309 (2014)
101. Lombi, E; Nowack, B; Baun, A; McGrath, S.P.: Evidence for effects of manufactured nanomaterials on crops is inconclusive. Proc. Natl. Acad. Sci. USA **109**(49), e3336 (2012)
102. Nevius, B.A.; Chen, Y.P.; Ferry, J.L.; Decho, A.W.: Surface functionalization effects on uptake of fluorescent polystyrene nanoparticles by model biofilms. Ecotoxicology **21**(8), 2205–2213 (2012)
103. Bagheri, H.; Ayazi, Z.; Es'haghi, A.; Aghakhani, A.: Reinforced polydiphenylamine nanocomposite for microextraction in packed syringe of various pesticides. J. Chromatogr. A **1222**, 13–21 (2012)
104. Ghormade, V.; Deshpande, M.V.; Paknikar, K.M.: Perspectives for nano-biotechnology enabled protection and nutrition of plants. Biotechnol. Adv. **29**(6), 792–803 (2011)
105. Khiew, P.; Chiu, W.; Tan, T.; Radiman, S.; Abd-Shukor, R.; Chia, C.H.: Capping effect of palm-oil based organometallic ligand towards the production of highly monodispersed nanostructured material. in: Palm Oil: Nutrition, Uses and Impacts, pp. 189–219. Nova Science (2011)
106. Aslani, F.; Bagheri, S.; Julkapli, N.M.; Juraimi, A.S.; Hashemi, F.S.G.; Baghdadi, A.: Effects of engineered nanomaterials on plants growth: an overview. Sci. World J. **2014**, 28 (2014). doi:10.1155/2014/641759
107. Elliott, K.C.: Nanomaterials and the precautionary principle. Environ. Health Perspect. **119**(6), A240–A245 (2011)
108. Lid'en, G.: The European Commission tries to define nanomaterials. Ann. Occup. Hyg. **55**(1), 1–5 (2011)
109. Potera, C.: Nanomaterials: transformation of silver nanoparticles in sewage sludge. Environ. Health Perspect. **118**(12), A526–A527 (2010)
110. Safiuddin, M.; Gonzalez, M.; Cao, J.W.; Tighe, S.L.: State of-the-art report on use of nanomaterials in concrete. Int. J. Pavement Eng. **15**(10), 940–949 (2014)
111. Zhou, X.; Torabi, M.; Lu, J.; Shen, R.; Zhang, K.: Nanostructured energetic composites: synthesis, ignition/combustion modeling, and applications. ACS Appl. Mater. Interfaces **6**(5), 3058–3074 (2014)
112. Baughman, R.H.; Zakhidov, A.A.; de Heer, W.A.: Carbon nanotubes—the route toward applications. Science **297**(5582), 787–792 (2002)
113. Lang, X.; Hirata, A.; Fujita, T.; Chen, M.: Nanoporous metal/oxide hybrid electrodes for electrochemical supercapacitors. Nat. Nanotechnol. **6**(4), 232–236 (2011)
114. Elmer, H.W.; White, C.J.: The use of metallic oxide nanoparticles to enhance growth of tomatoes and eggplants in disease infected soil or soilless medium. Environ. Sci. Nano **3**, 1072–1079 (2016)
115. Pariona, N.; Martinez, A.I.; Hdz-García, H.M.; Cruz, L.A.; Hernandez-Valdes, A.: Effects of hematite and ferrihydrite nanoparticles on germination and growth of maize seedlings. Saudi J. Biol. Sci. **24**(7), 1547–1554 (2017)
116. Rui, M.; Ma, C.; Hao, Y.; Guo, J.; Rui, Y.; Tang, X.; Zhao, Q.; Fan, X.; Zhang, Z.; Hou, T.; Zhu, S.: Iron oxide nanoparticles as a potential iron fertilizer for peanut (Arachishypogaea). Front. Plant Sci. **7**, 815 (2016)
117. Li, J.; Yi, Y.; Cheng, X.; Zhang, D.; Irfan, M.: Study on the effect of magnetic field treatment of newly isolated Paenibacillus sp. Bot. Stud. **56**, 2 (2015)
118. Zhongzhou, Yang; Chen, Jing; Dou, Runzhi; Gao, Xiang; Mao, Chuanbin; Wang, Li: Assesment of phytotoxicity of metal oxide nanoparticles on two crop plants, Maize (*Zea mays* L.) and Rice (*Oryza sativa* L.). Int. J. Environ. Res. Public Health **12**, 15100–15109 (2015)
119. Niederberger, M.: Nonaqueous sol–gel routes to metal oxide nanoparticles. Acc. Chem. Res. **40**(9), 793–800 (2007)
120. Franke, M.E.; Koplin, T.J.; Simon, U.: Metal and metal oxide nanoparticles in chemiresistors: does the nanoscale matter? Small **2**(1), 36–50 (2006)
121. Zhu, H.; Han, J.; Xiao, J.Q.; Jin, Y.: Uptake, translocation, and accumulation of manufactured iron oxide nanoparticles by pumpkin plants. J. Environ. Monit. **10**(6), 713–717 (2008)
122. Besson-Bard, A.; Gravot, A.; Richaud, P.; Auroy, P.; Duc, C.; Gaymard, F.; Taconnat, L.; Renou, J.P.; Pugin, A.; Wendehenne, D.: Nitric oxide contributes to cadmium toxicity in arabidopsis by promoting cadmium accumulation in roots and by up-regulating genes related to iron uptake. Plant Physiol. **149**(3), 1302–1315 (2009)
123. Stephan, M.K.: Iron oxide dissolution and solubility in the presence of sidrophores. Aquat. Sci. **66**(1), 3–18 (2004)
124. Bombin, S.; LeFebvre, M.; Sherwood, J.; Xu, Y.; Bao, Y.; Ramonell, K.M.: Developmental and reproductive effects of iron oxide nanoparticles in *Arabidopsis thaliana*. Int. J. Mol. Sci. **16**(10), 24174–24193 (2015)
125. Li, J.; Chang, P.R.; Huang, J.; Wang, Y.; Yuan, H.; Ren, H.: Physiological effect of magnetic iron oxide nanoparticles toward watermelon. J. Nanosci. Nanotechnol. **13**, 5561–5567 (2013)
126. O'Brien, R.D.: Toxic Phosphorus Esters. Chemistry, Metabolism, and Biological Effects. Academic Press, New York (1960)
127. Chauhan, N.; Pundir, C.S.: An amperometric biosensor based on acetylcholinesterase immobilized onto iron oxide nanoparticles/multi-walled carbon nanotubes modified gold electrode for measurement of organophosphorus insecticides. Anal. Chim. Acta **701**, 66–74 (2011)
128. Bhat, S.S.; Qurashi, A.; Khanday, F.A.: ZnO nanostructures based biosensors for cancer and infectious disease applications: perspectives, prospects and promises. Trends Anal. Chem. **86**, 1–13 (2017)

129. Jordan, A.; Wust, P.; Scholz, R.; Tesche, B.; Fahling, H.; Mitrovics, T.; Vogl, T.; Cervos-Navarro, J.; Felix, R.: Cellular uptake of magnetic fluid particles and their effects on human adenocarcinoma cells exposed to AC magnetic fields in vitro. Int. J. Hyperthermia **12**(6), 705–722 (1996)
130. Ulbrich, K.; Holá, K.; Šubr, V.; Bakandritsos, A.; Tuček, J.; Zbořil, R.: Targeted drug delivery with polymers and magnetic nanoparticles: covalent and noncovalent approaches, release control, and clinical studies. Chem. Rev. **116**(9), 5338–5431 (2016)
131. Parray, A.A.; Baba, R.A.; Bhat, H.F.; Wani, L.; Mokhdomi, T.A.; Mushtaq, U.; Bhat, S.S.; Kirmani, D.; Kuchay, S.; Wani, M.M.; Khanday, F.A.: MKK6 is upregulated in human esophageal, stomach, and colon cancers. Cancer Invest. **32**(8), 416–422 (2014)
132. Bashir, M.; Kirmani, D.; Bhat, H.F.; Baba, R.A.; Hamza, R.; Naqash, S.; Wani, N.A.; Andrabi, K.I.; Zargar, M.A.; Khanday, F.A.: P66shc and its downstream Eps8 and Rac1 proteins are upregulated in esophageal cancers. Cell Commun. Signal. **8**, 13 (2010)
133. Mushtaq, U.; Baba, R.A.; Parray, A.A.; Bhat, H.F.; Saleem, S.S.; Manzoor, U.; Kuchay, S.; Wani, L.; Khanday, F.A.: Mitogen activated protein kinase kinase-4 upregulation is a frequent event in human stomach and colon cancers. J. Enzymol. Metabol. **1**(1), 103 (2014)
134. Kemmner, W.; Moldenhauer, G.; Schlag, P.; Brossmer, R.: Separation of tumor cells from a suspension of dissociated human colorectal carcinoma tissue by means of monoclonal antibody-coated magnetic beads. J. Immunol. Methods **147**(2), 197–200 (1992)
135. Kiessling, A.A., Anderson , S.C.: Human Embryonic Stem Cells. Jones and Bartlett, Boston, MA (2003)
136. Bulte, J.W.; Douglas, T.; Witwer, B.; Zhang, S.C.; Strable, E.; Lewis, B.K.; Zywicke, H.; Miller, B.; van Gelderen, P.; Moskowitz, B.M.; Duncan, I.D.; Frank, J.A.: Magnetodendrimers allow endosomal magnetic labeling and in vivo tracking of stem cells. Nat. Biotechnol. **19**, 1141–1147 (2001)
137. Tosi, G.; Costantino, L.; Rivasi, F.; Ruozi, B.; Leo, E.; Vergoni, A.V.; Tacchi, R.; Bertolini, A.; Vandelli, M.A.; Forni, F.: Targeting the central nervous system: in vivo experiments with peptide-derivatized nanoparticles loaded with Loperamide and Rhodamine-123. J. Control. Release **122**, 1–9 (2007)
138. Vail, D.M.; Amantea, M.A.; Colbern, G.T.; Martin, F.J.; Hilger, R.A.; Working, P.K.: Pegylated liposomal doxorubicin: proof of principle using preclinical animal models and pharmacokinetic studies. Semin. Oncol. **31**, 16–35 (2004)
139. Wang, Y.; Cui, H.; Li, K.; Sun, C.; Du, W.; Cui, J.; Zhao, X.; Chen, W.: A magnetic nanoparticle-based multiple-gene delivery system for transfection of porcine kidney cells. PLoS One **9**, e102886 (2014)
140. Krotz, F.; Wit, C.; Sohn, H.Y.; Zahler, S.; Gloe, T.; Pohl, U.; Plank, C.: Magnetofection-a highly efficient tool for antisense oligonucleotide delivery in vitro and in vivo. Mol. Ther. **7**, 700–710 (2003)
141. Miller, M.M.; Prinz, G.A.; Cheng, S.F.; Bounnak, S.: Detection of a micron-sized magnetic sphere using a ring-shaped anisotropic magnetoresistance-based sensor: a model for a magnetoresistance-based biosensor. Appl. Phys. Lett. **81**, 2211 (2002)
142. Nor, N.M.; Lockman, Z.; Razak, K.A.: Study of ITO glass electrode modified with iron oxide nanoparticles and Nafion for glucose biosensor application. Procedia Chem. **3**, 116 (2016)
143. Kaushik, A.; Khan, R.; Solanki, P.R.; Pandey, P.; Alam, J.; Ahmad, S.; Malhotra, B.D.: Iron oxide nanoparticles-chitosan composite based glucose biosensor. Biosens. Bioelectron. **24**, 676–683 (2008)
144. AlSalhi, A.M.S.; Atif, M.; Ansari, A.A.; Israr, M.Q.; Sadaf, J.R.; Ahmed, E.; Nur, O.; Willander, M.: Potentiometric urea biosensor utilizing nanobiocomposite of chitosan-iron oxide magnetic nanoparticles. J. Phys. Conf. Ser. **414**, 012024 (2013)
145. Hutter, E.; Cha, S.; Liu, J.-F.; Park, J.; Yi, J.; Fendler, J.H.; Roy, D.: Role of substrate metal in gold nanoparticle enhanced surface plasmon resonance imaging. J. Phys. Chem. B **105**, 8–12 (2001)
146. Ansari, M.I.H.; Hassan, S.; Qurashi, A.; Khanday, F. A.: Microfluidic-integrated DNA nanobiosensors. Biosens. Bioelectron. **85**, 247–260 (2016)
147. Ambashta, R.D.; Sillanpaa, M.: Water purification using magnetic assistance: a review. J. Hazard. Mater. **180**, 38–49 (2010)
148. Pradeep, T.: Noble metal nanoparticles for water purification: a critical review. Thin Solid Films **517**, 6441–6478 (2009)
149. Hu, J.; Lo, M.C.I.; Chen, G.H.: Performance and mechanism of chromate (VI) adsorption by δ-FeOOH-coated maghemite (γ-Fe_2O_3) nanoparticles. Sep. Purif. Technol. **58**, 76–82 (2007)
150. Mirabedini, M.; Kassaee, M.Z.; Poorsadeghi, S.: Novel magnetic chitosan hydrogel film, cross-linked with glyoxal as an efficient adsorbent for removal of toxic Cr(VI) from water. Arab. J. Sci. Eng. **42**, 115–124 (2017)
151. Mahdavian, A.R.; Mirrahimi, M.A.S.: Efficient separation of heavy metal cations by anchoring polyacrylic acid on superparamagnetic magnetite nanoparticles through surface modification. Chem. Eng. J. **159**, 264–271 (2010)
152. Nadejdea, C.; Neamtua, M.; Schneiderb, R.J.; Hodoroabab, V.D.; Ababeic, G.; Panneb, U.: Catalytical degradation of relevant pollutants from waters using magnetic nanocatalysts. Appl. Surf. Sci. **352**, 42–48 (2015)
153. Bhattacharya, K.; Parasar, D.; Mondal, B.; Deb, P.: Mesoporous magnetic secondary nanostructures as versatile adsorbent for efficient scavenging of heavy metals. Sci. Rep. **25**, 1–9 (2015)
154. Rauf, M.A.; Ali, L.; Sadig, M.S.A.Y.; Ashraf, S.S.; Hisaindee, S.: Comparative degradation studies of malachite green and thiazole yellow G and their binary mixture using UV/H_2O_2. Desalin. Wat. Treat. **57**(18), 8336–8342 (2016)
155. Khataee, A.; Gohari, S.; Fathinia, M.: Modification of magnetite ore as heterogeneous nanocatalyst for degradation of three textile dyes: simultaneous determination using MCR-ALS, process optimization and intermediate identification. J. Taiwan Inst. Chem. Eng. **65**, 172–184 (2016)
156. Khataee, A.; Taseidifar, M.; Khorram, S.; Sheydaei, M.; Joo, S.W.: Preparation of nanostructured magnetite with plasma for degradation of a cationic textile dye by the heterogeneous Fenton process. J. Taiwan Inst. Chem. Eng. **53**, 132–139 (2015)
157. Khosravi, M.; Azizian, S.: Synthesis of Fe_3O_4 flower-like hierarchical nanostructures with high adsorption performance toward dye molecules. Colloids Surface Physicochem. Eng. Asp. **482**, 438–446 (2015)
158. Jiao, C.; Wang, Y.; Li, M.; Wu, Q.; Wang, C.; Wang, Z.: Synthesis of magnetic nanoporous carbon from metal-organic framework for the fast removal of organic dye from aqueous solution. J. Magn. Magn. Mater. **407**, 24–30 (2016)
159. Jiang, X.; Yu, J.; Chen, X.; Wang, D.; Liu, L.: Adsorption and removal of malachite green from aqueous solution using magnetic cyclodextrin-graphene oxide nanocomposites as adsorbents. Colloids Surface Physicochem. Eng. Asp. **66**, 166–173 (2015)
160. Le, T.H.; Kim, S.J.; Bang, S.H.; Lee, S.H.; Choi, Y.W.; Kim, P.; Kim, Y.H.; Min, J.: Phenol degradation activity and reusability of *Corynebacterium glutamicum* coated with NH_2-functionalized silica-encapsulated Fe_3O_4 nanoparticles. Bioresour. Technol. **104**, 795–798 (2012)
161. Zhang, S.X.; Niu, H.Y.; Hu, Z.J.; Cai, Y.Q.; Shi, Y.L.: Nanomaterials in pollution trace detection and environmental improvement. J. Chromatogr. A **1217**, 4757–4764 (2010)
162. Huang, Y.; Fulton, A.N.; Keller, A.A.: Simultaneous removal of PAHs and metal contaminants from water using magnetic

nanoparticle adsorbents. Sci. Total Environ. **571**, 1029–1036 (2016)
163. Abdullah, M.M.S.; Al-Lohedan, H.A.; Atta, A.M.: Novel magnetic iron oxide nanoparticles coated with sulfonated asphaltene as crude oil spill collectors. RSC Adv. **6**, 59242–59249 (2016)
164. Zhu, X.; Tian, S.; Cai, Z.: Toxicity assessment of iron oxide nanoparticles in Zebrafish (*Danio rerio*) early life stages. PLoS ONE **7**, e46286 (2012)
165. Barhoumi, L.; Dewez, D.: Toxicity of superparamagnetic iron oxide nanoparticles on green alga *Chlorella vulgaris*. BioMed Res. Int. **2013**, 647974 (2013)